Geochemistry Geophysics Geosystems G3
AN ELECTRONIC JOURNAL OF THE EARTH SCIENCES
Published by AGU and the Geochemical Society

Article
Volume 5, Number 8
24 August 2004
Q08006, doi:10.1029/2004GC000717
ISSN: 1525-2027

Growth and collapse of Waianae Volcano, Hawaii, as revealed by exploration of its submarine flanks

Michelle L. Coombs
U.S. Geological Survey, 345 Middlefield Road, MS 910, Menlo Park, California 94025, USA

Now at Alaska Volcano Observatory, U.S. Geological Survey, 4200 University Drive, Anchorage, Alaska 99508, USA (mcoombs@usgs.gov)

David A. Clague
Monterey Bay Aquarium Research Institute, Moss Landing, California 95039, USA

Gregory F. Moore
Department of Geology and Geophysics, University of Hawai'i, Honolulu, Hawaii 96822, USA

Brian L. Cousens
Department of Earth Sciences, Carleton University, Ottawa, Ontario, Canada K1S 5B6

[1] Wai'anae Volcano comprises the western half of O'ahu Island, but until recently little was known about the submarine portion of this volcano. Seven new submersible dives, conducted in 2001 and 2002, and multibeam bathymetry offshore of Wai'anae provide evidence pertaining to the overall growth of the volcano's edifice as well as the timing of collapses that formed the Wai'anae slump complex. A prominent slope break at ~1400 mbsl marks the paleoshoreline of Wai'anae at the end of its shield-building stage and wraps around Ka'ena Ridge, suggesting that this may have been an extension of Wai'anae's northwest rift zone. Subaerially erupted tholeiitic lavas were collected from a small shield along the crest of Ka'ena Ridge. The length of Wai'anae's south rift zone is poorly constrained but reaches at least 65 km on the basis of recovered tholeiite pillows at this distance from the volcano's center. Wai'anae's growth was marked by multiple collapse and deformation events during and after its shield stage, resulting in the compound mass wasting features on the volcano's southwest flank (Wai'anae slump complex). The slump complex, one of the largest in Hawai'i, covering an area of ~5500 km^2, is composed of several distinct sections on the basis of morphology and the lithologies of recovered samples. Two dives ascended the outer bench of the slump complex and collected predominantly low-S tholeiites that correlate with subaerial lavas erupted early during the volcano's shield stage, from 3.9 to 3.5 Ma. Pillow lavas from the outer bench have Pb, Sr, and Nd isotopic values that overlap with previously published subaerial Wai'anae lavas. On the basis of the compositions of the recovered samples, the main body of the slump complex, as represented by the outer bench, probably formed during and shortly after the early shield stage. To the southwest of the outer bench lies a broad debris field on the seafloor, interpreted to have formed by a catastrophic collapse event that breached the outer bench. A dive within the debris field recovered subaerially derived volcaniclastic rocks; analyzed glasses are tholeiitic and resemble early shield stage compositions. The breach may have then been filled by slumping material from the main volcanic edifice. Finally, atop the northern main body of the slump is a rotated landslide block that detached from the proximal part of Ka'ena Ridge after the volcano's late shield stage (3.2 to 3.0 Ma). From the inner scarp of this block we recovered subaerially erupted tholeiitic pillow breccias and hyaloclastites that are systematically higher in alkalis and more fractionated than those collected from the outer bench. These rocks correlate compositionally with late shield-stage subaerial Kamaile'unu lavas. None of the collected slump complex samples correlate with alkalic subaerial postshield lavas. Volcaniclastic rocks and glass disseminated in pelagic sediment, collected from north of Ka'ena Ridge, originated from Wai'anae's postshield stage and Ko'olau's shield stage, respectively.

Copyright 2004 by the American Geophysical Union

Components: 15,378 words, 13 figures, 5 tables.

Keywords: Hawaii; landslide; O‘ahu; submarine; volcaniclastic; Wai‘anae.

Index Terms: 3045 Marine Geology and Geophysics: Seafloor morphology and bottom photography; 3655 Mineralogy and Petrology: Major element composition; 8499 Volcanology: General or miscellaneous.

Received 12 February 2004; **Revised** 22 May 2004; **Accepted** 22 June 2004; **Published** 24 August 2004.

Coombs, M. L., D. A. Clague, G. F. Moore, and B. L. Cousens (2004), Growth and collapse of Waianae Volcano, Hawaii, as revealed by exploration of its submarine flanks, *Geochem. Geophys. Geosyst.*, *5*, Q08006, doi:10.1029/2004GC000717.

1. Introduction

[2] Landslides are recognized as an important feature of Hawaiian volcanoes [*Moore et al.*, 1989], as well as potentially the most catastrophic geologic hazard related to the Hawaiian Islands due to their capacity for generating megatsunamis [*Ward*, 2001; *Satake et al.*, 2002; *McMurtry et al.*, 2004]. Recent study of Hawaiian landslide deposits, in particular on the flanks of Kīlauea and Mauna Loa volcanoes, has led to insights into their structure and emplacement mechanisms, timing of landslide events with respect to volcano growth, and overall petrogenetic evolution [*Lipman et al.*, 2002, 2003; *Sisson et al.*, 2002; *Morgan and Clague*, 2003; *Morgan et al.*, 2003; *Yokose and Lipman*, 2004]. For older Hawaiian volcanoes, landslide deposits preserve information about volcano evolution that has likely been lost from the onland record due to burial and subsidence of the subaerial portion of the edifice [e.g., *Shinozaki et al.*, 2002; *Tanaka et al.*, 2002].

[3] Landslides can be placed into two broad categories: far-traveled debris avalanches and larger, more coherent slumps. Ko‘olau Volcano collapsed to form the Nu‘uanu landslide on the east side of O‘ahu, the largest example of a debris avalanche in Hawaii, whereas the Hilina slump on the south flank of Kīlauea is a classic example of a slowly deforming slump [*Moore et al.*, 1989]. The geologic histories of individual Hawaiian volcanoes likely involve an array of mass movement processes, ranging from near steady state volcano spreading [e.g., *Borgia and Treves*, 1992] to catastrophic collapse events.

[4] Wai‘anae slump, a morphologically complex landslide off the SW of the island of O‘ahu, is one of the largest submarine features on the flanks of the Hawaiian Islands. First recognized during the GLORIA surveys in the 1980s [*Hussong et al.*, 1987; *Moore et al.*, 1989], it has recently been mapped in detail by several SeaBeam surveys, including those by the Japan Marine Science and Technology Center (JAMSTEC) in 2001 and 2002. During the same cruises, as well as during a cruise by the Monterey Bay Aquarium Research Institute (MBARI) in 2001, submersible and remotely operated vehicle (ROV) dives provided first hand observations and samples of the slump and surrounding areas. Investigating this relatively unknown landslide provides new information regarding processes of volcano deformation and collapse. Study of Wai‘anae Volcano has previously been limited to on-land rocks, and the submarine sampling and observations described here are the first for this volcanic center.

[5] In this paper, we combine geologic observations made during dives and SeaBeam bathymetric mapping to better understand the structure and emplacement of the Wai‘anae landslide deposits, and overall development of the submarine portions of Wai‘anae Volcano. We also describe the compositions and textures of samples collected from the Wai‘anae slump as well as to the north of Ka‘ena Ridge. By comparing compositions of rocks within the slump to stratigraphically constrained subaerial samples, we place constraints on the timing of slump emplacement. Compositions of rocks sampled along the entire slump suggest that this feature may have been derived in its entirety from Wai‘anae Volcano. Morphology and compositional variation within the slump suggest a history marked by multiple, possibly rapid, collapse events in addition to steady-state flank deformation during the volcano’s shield stage.

2. Geologic Background

[6] Deeply eroded Wai‘anae Volcano comprises the western half of the island of O‘ahu. Subaerially preserved products of the volcano, the Wai‘anae

Volcanics, are divided into four members: Lualualei, Kamaileʻunu, Palehua, and Kolekole [*Presley et al.*, 1997; *Sinton*, 1986]. Its shield stage has been dated from 3.93 to 3.08 Ma using unspiked K-Ar methods, and has been broken into two members [*Guillou et al.*, 2000]. The oldest exposed shield-stage rocks, tholeiites found along the base of ridges near the shoreline, are the Lualualei Member (3.93 to 3.54 Ma). These early shield-stage lavas are relatively undifferentiated and strongly tholeiitic [*Zbinden and Sinton*, 1988]. Later shield-building and caldera-filling lavas comprising the Kamaileʻunu Member (3.57 to 3.08 Ma) are more heterogeneous than those of the Lualualei Member, and include plagioclase-phyric tholeiitic basalts, alkali olivine basalts, and plagioclase-phyric basaltic hawaiites, with alkalic compositions becoming common high in the unit. Kamaileʻunu tholeiites can be distinguished from earlier Lualualei basalts by their higher incompatible element concentrations and more fractionated nature [*Sinton*, 1986; *Zbinden and Sinton*, 1988]. Postshield volcanism first produced primarily aphyric hawaiite (Palehua Member) from 3.06 to 2.98 Ma as dated by K-Ar [*Presley et al.*, 1997]. Palehua Member hawaiites are unconformably overlain by small volumes of alkali basalt (Kolekole Member) that erupted from 2.97 to 2.90 Ma; the hiatus between the two members is probably less than 10,000 years [*Presley et al.*, 1997]. *Presley et al.* [1997] suggest that the Waiʻanae slump may have occurred during the brief interval between the Palehua and Kolekole Members. The unloading caused by such an event could have led to the curious transition from hawaiite to alkali basalt as the volcano moved through its postshield stage.

[7] Other volcanism was occurring in the region during Waiʻanae's growth. Neighboring Koʻolau volcano comprises the eastern half of Oʻahu. The oldest dated lavas from the volcano yield $^{40}Ar/^{39}Ar$ plateau ages of ~2.9 Ma [*Haskins and Garcia*, 2004], and dates for the shield stage range to 1.8 Ma (summarized by *Clague and Dalrymple* [1987]). The Southwest Oʻahu Volcanic Field is a series of alkalic lavas and cones on the seafloor southwest of the island [*Holcomb and Robinson*, 2004; *Takahashi et al.*, 2001]. Preliminary dating of lavas from the field yields ages of ~3 Ma [*Noguchi and Nakagawa*, 2003], though MnO rind thicknesses suggest that some lavas in the field may be considerably younger [*Moore and Clague*, 2004]. Other isolated alkalic lavas and vents are present on the seafloor between Oʻahu and Kauaʻi [*Clague et al.*, 2003].

[8] Waiʻanae Volcano has two well-developed subaerial rift zones: a prominent one to the northwest and a more diffuse one to the south; these are defined by concentrations of subparallel dikes [*Stearns*, 1939; *Zbinden and Sinton*, 1988] and an elongated gravity high [*Strange et al.*, 1965a]. The southern rift zone migrated from west to east during the volcano's shield stage [*Zbinden and Sinton*, 1988]. Undifferentiated tholeiites from early in the shield-stage are more abundant in the rift zones, while differentiated theoliites and alkalic lavas from the late shield stage occur both in the rift zones and within the caldera [*Zbinden and Sinton*, 1988].

[9] Compared to the volcano's well-studied subaerial edifice, little was previously known about its submarine flanks. The Waiʻanae slump (Figures 1 and 2) is the dominant submarine feature off the west coast of Oʻahu Island, and was originally termed West Oʻahu Giant Landslide [*Hussong et al.*, 1987]. It was renamed by *Moore et al.* [1989], who used GLORIA sonar data to determine that it covers an area of approximately 6,000 km^2, and consists of several coherent blocks spaced 5–20 km apart, separated by transverse scarps. The northern portion of the slump lies downslope of Kaʻena Ridge, the central portion of the slump is directly downslope from Waiʻanae Volcano's deeply eroded summit region, and the southern part of the slump lies downslope of a 600-m-deep shelf between Oʻahu and Penguin Bank. A conservative volume estimate for the slump is 6,000–12,000 km^3, based on profiles of 1–2 km thickness [*Presley et al.*, 1997]. On the basis of the width of the scarps at the slump's head, it has been suggested that it formed during multiple slide events [*Moore et al.*, 1989], but it has been unclear how much of the slump consists of material from Waiʻanae Volcano, or even how far northwest and south the volcano's original edifice extended.

[10] Kaʻena Ridge is a 35–55 km wide submarine feature that extends 75–100 km northwest from Kaʻena Point off westernmost Oʻahu (Figure 1). Morphologically it resembles the large Hāna Ridge, the east rift zone of Haleakalā volcano, but there are two cones near the western end of Kaʻena Ridge, suggesting that it may, at least in part, be a separate center instead of simply a rift zone of Waiʻanae [*Smith*, 2002]. Waialu Ridge, which exhibits more typical submarine rift zone morphology, extends to the northwest from the north flank of Kaʻena Ridge. Between Waialu Ridge and the island of Oʻahu, Kaʻena Ridge's north flank is marked by two benches, the easternmost of which encloses a sediment-filled basin. Outboard of the benches are

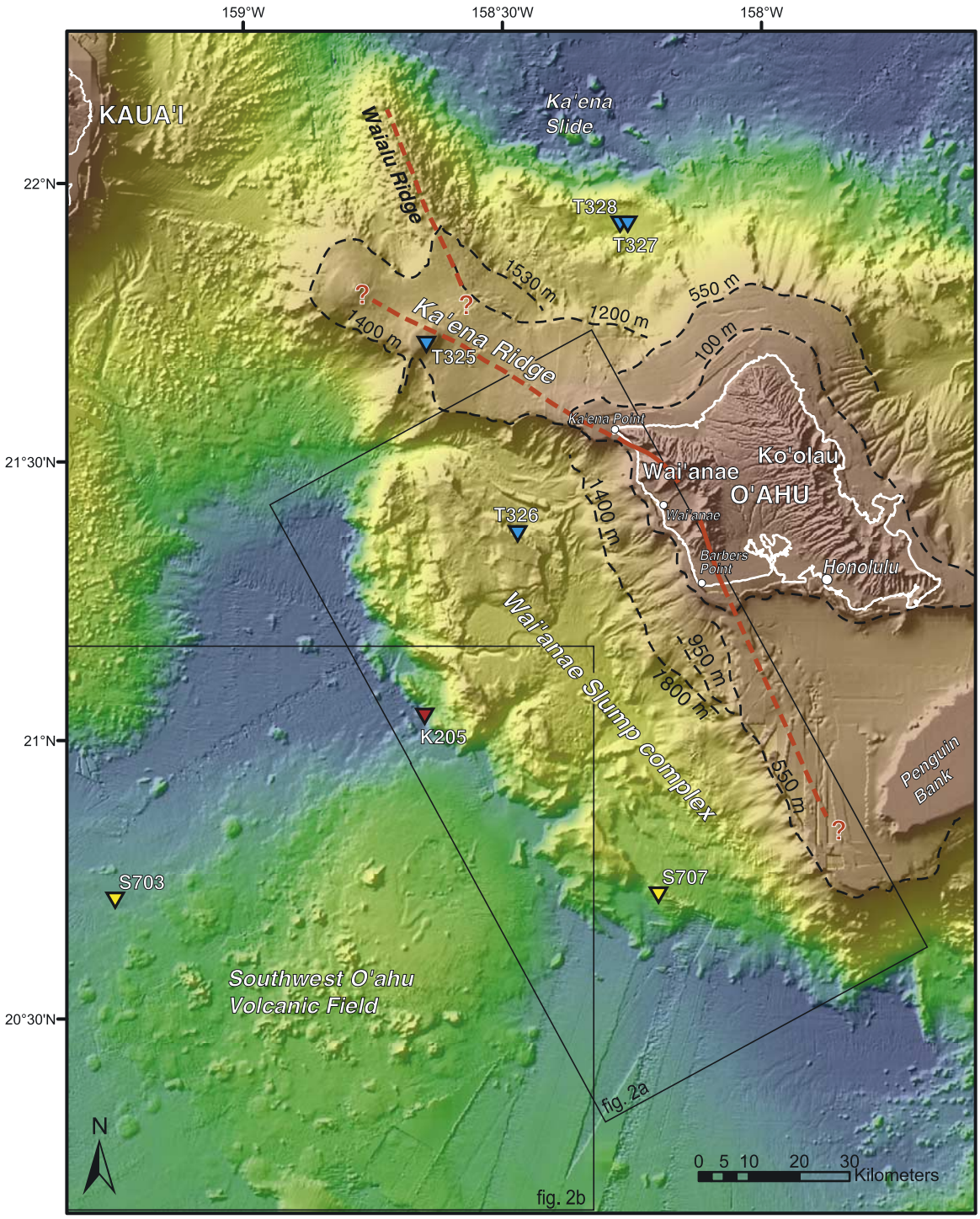

Figure 1. Shaded relief map of western O‘ahu Island and surrounding bathymetric features. Location of ROV and submersible dives shown in blue (*Tiburon*), red (*Kaiko*), and yellow (*Shinkai 6500*). Locations of Figures 2a and 2b are indicated by boxes. Bold, dashed lines show the location of submarine terraces discussed in text. Rift zones of Wai‘anae Volcano are shown in red, and dashed where inferred.

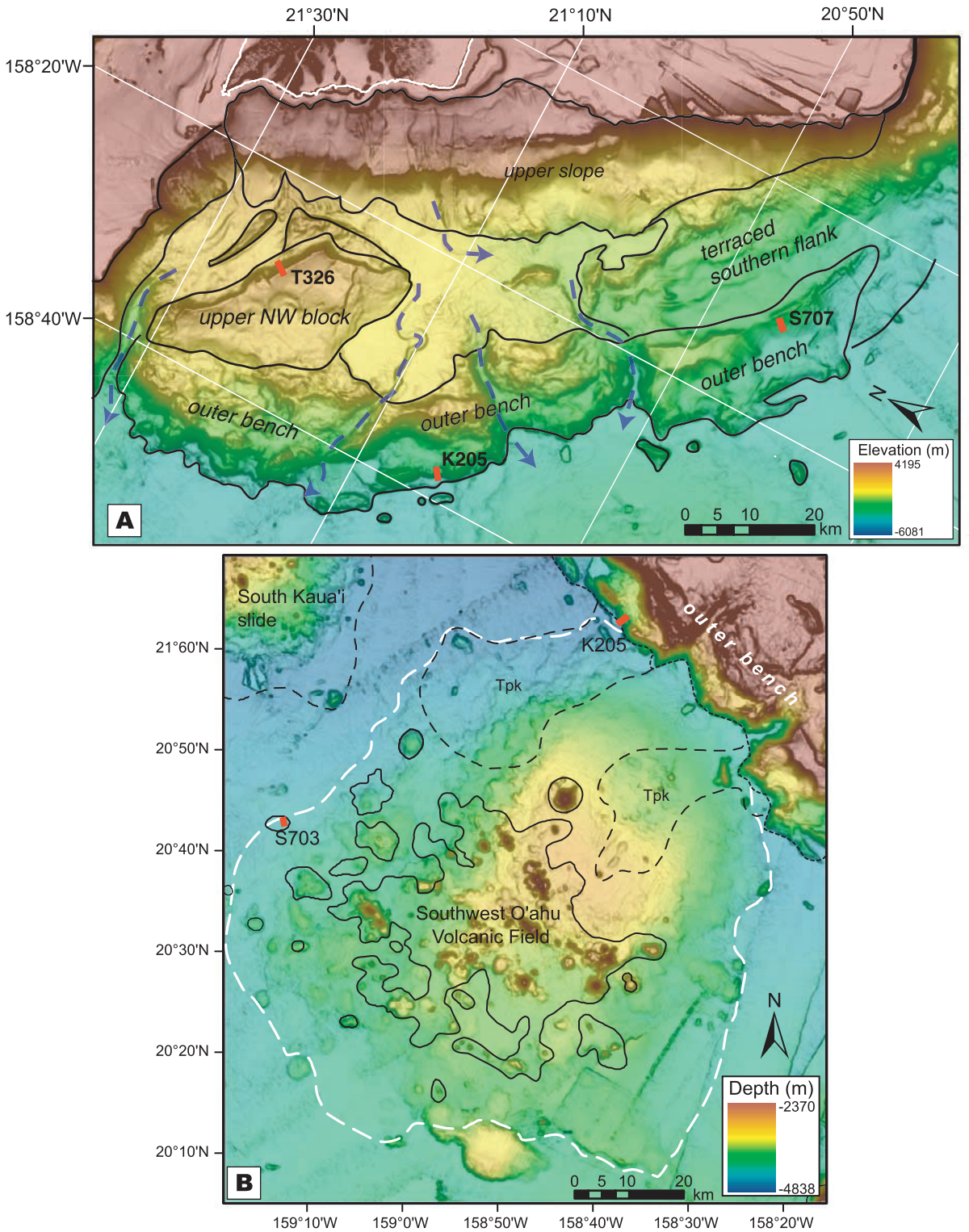

Figure 2. (a) Depth-colored slope map of the Wai'anae slump complex, with delineated areas discussed in text. Blue dashed arrows show locations of sediment channels. O'ahu Island outlined in white. (b) Slope map of debris field, outlined in white dashed line. Black, short-dashed lines show outer bench, and long-dashed lines show landslide regions defined by *Holcomb and Robinson* [2004] using GLORIA sidescan sonar data, including the South Kaua'i landslide and "Pliocene-age fine debris avalanche" (Tpk). Solid black lines delineate areas of the seafloor covered by the Southwest O'ahu Volcanic Field, modified from *Holcomb and Robinson* [2004].

scattered blocks that extend more than 90 km onto the seafloor. This region has been mapped as the Kaʻena landslide [*Moore et al.*, 1989; *Holcomb and Robinson*, 2004].

3. Morphology of Waiʻanae's Submarine Flanks

[11] We conducted systematic multibeam bathymetry surveys over the southwest flank of Oʻahu Island using SeaBeam 2112 sonar mapping systems during the 2001 R/V *Kairei* and 2002 R/V *Yokosuka* cruises. These systems are described by *Smith et al.* [2002]. We have also incorporated other regional multibeam data collected by ships of Scripps Institution of Oceanography and the University of Hawaiʻi. Data processing included editing (deleting bad data from individual ping files, elimination of track crossing discrepancies, etc.) and gridding at 100 m. All processing used MB-System software [*Caress and Chayes*, 1996].

[12] Previous surveys have revealed the dominant features on the seafloor surrounding Waiʻanae: Kaʻena Ridge lies to the northwest of Oahu, the Waiʻanae slump is to the west-southwest of the island, and a shallow platform connects the southern flank of the volcano to Penguin Bank to the south. The new bathymetric surveys reveal these and other features in much greater detail (Figure 1). Below we identify prominent slope breaks along Waiʻanae's flank, and describe several distinct morphological terranes within the Waiʻanae slump.

3.1. Submerged Terraces

[13] Two types of terraces and slope breaks are recognized on the submarine flanks of the Hawaiian Islands. Breaks in slope on the submarine flanks of the islands commonly mark paleotransitions between the subaerial and steeper submarine portions of a volcano's edifice [*Mark and Moore*, 1987], and are found in deeper water for older volcanoes due to subsidence [*Moore*, 1987]. Another type of slope break on the islands' submarine flanks are drowned coral reefs, which also mark paleo sea levels [*Moore and Campbell*, 1987]. Both types of slope breaks are present on the submarine portion of Waiʻanae (Figure 1). The shallowest of these wraps around the island of Oʻahu at a depth of ~100 m, and like terraces near this depth around other islands in the chain is composed of several overlapping reefs drowned due to glacioeustatic sea level fluctuations in the late Pleistocene [*Moore*, 1987]. Off the north coast of Oʻahu, a prominent slope break at 550 m water depth probably marks the end of shield building for Koʻolau volcano (1.8 Ma [*Langenheim and Clague*, 1987]). This terrace also occurs just below the widespread carbonate platform between Oʻahu and Penguin Bank. Just south of Barbers Point is a short terrace at 950 m water depth. To the south it terminates as it approaches the 550 m platform and to the northwest it is buried by sediment downslope of the eroding subaerial edifice.

[14] The deepest slope break is a widespread terrace that wraps around Kaʻena Ridge and below the southwest coast of Oʻahu. This terrace is at ~1200 m along the northern side of Kaʻena Ridge, 1340 m at the ridge's farthest extent, and then shallows to near sea level as it wraps around the southern half of the ridge and approaches Kaʻena Point. The terrace is reestablished at 1400 m depth just southeast of the scarp and then deepens to 1800 m to the southeast, where it ends just below the termination of the 950 m slope break. Such tilting of a once-horizontal terrace is likely due to increased loading of the crust by the broader part of the Hawaiian Ridge to the southeast [*Moore*, 1987]. We interpret this widespread feature as the submerged shoreline of Waiʻanae at the end of its shield-building stage, at 3.08 Ma [*Guillou et al.*, 2000]. This suggests that ~650 m of subsidence occurred during the interval between the end of shield stages for Waiʻanae and Koʻolau volcanoes, approximately 1.3 m.y.

3.2. Waiʻanae Slump Complex

[15] The Waiʻanae slump is one of the largest mass-wasting features on the flanks of the Hawaiian Islands, covering an area of approximately 5500 km^2. The slump reveals features typical of a slump-type landslide, as well as unusual features indicative of a complicated history. The steep scarp at its toe and transverse faults that cut it into a few large blocks generally wider than they are long are characteristics shared by slumps such as Hilina, Laupahoehoe, and Hāna [e.g., *Smith et al.*, 1999, 2002; *Eakins and Robinson*, 2002]. Unlike some other slumps, it lacks a well-defined amphitheater at its head. Because of the great size and morphological complexity of this feature, we propose that a more appropriate term is the Waiʻanae slump complex. Within this broad feature several smaller areas merit special attention.

3.2.1. Outer Bench

[16] The outermost segments of the slump are here termed the outer bench (Figure 2a). The outer

bench is similar in morphology to the midslope bench (“outer bench” of *Morgan et al.* [2003]) on Kīlauea’s submarine south flank [*Moore and Peck*, 1965; *Lipman et al.*, 1988; *Chadwick et al.*, 1993; *Smith et al.*, 1999] The outer bench varies greatly in morphology along its extent. The northernmost section, from 21°10′ to 21°30′N, features hummocky terrain marked by irregularly placed and shaped blocks, 4 to 11 km in length with up to 400 m of relief. The outer boundary of the northern portion of the outer bench is irregular, and its more proximal edge is obscured by an overlying upper block. This section of the bench is bounded on either side by deep canyons.

[17] To the south of 21°10′, the outer bench consists of three distinct sections: two parallel segments, separated by a ~20 km-wide embayment. In the parallel segments, a prominent ridge parallels the slump’s outer edge. Beyond, smaller, parallel ridges form the slump’s outermost boundary and are partially infilled by sediment. Outboard of these, a few isolated, also elongate blocks rest directly on the seafloor, but no blocky debris fields are present outboard of these sections. In contrast, the section of the outer bench marked by an embayment (approximately 20°50′ to 21°N) consists of three roughly subparallel ridges, convex to the southwest (Figure 2). This section has more rugged morphology than the sections of the outer bench to either side. It is bounded on both sides by canyons that are fed from the sediment-filled basins atop the slump.

3.2.2. Debris Field

[18] Outboard of the main body of the Wai‘anae slump is a large debris field on the abyssal seafloor, covering an area of at least 2700 km^2 (Figure 2b). This debris field as a whole does not show up on GLORIA side scan sonar imagery, but two lobe-shaped high-reflectivity fields within the apparent margins of the deposit were mapped by *Holcomb and Robinson* [2004] as fine-grained landslide and may be portions of the debris field that were not subsequently covered by sediment. The debris field has lobate edges but fewer large blocks than other slides, such as the Alika 2 slide from Mauna Loa [*Lipman et al.*, 1988] or the South Kaua‘i slide just to the north [*Moore et al.*, 1989]. The thickness of the deposit is not well constrained, but it may be up to 700 m thick based simply on the difference in water depth between its highest point and the surrounding moat. Some of this thickness, however, may be attributed to sills associated with the Southwest O‘ahu Volcanic Field, which partially covers the deposit. The extent of the debris field is similarly hard to delineate. Dive S703, discussed below, encountered volcaniclastic debris, despite being in an area where SeaBeam did not discern any obvious debris. Thus the boundaries shown in Figure 2b are approximate.

[19] The headwall scarp that fed the debris field is not observed. The northeastern edge of the debris field coincides with the distinct reentrant along the outer bench, through which debris have been channeled (Figures 1 and 2). The debris field is broadly dome-shaped, with a bathymetric low closest to the reentrant. This could be due to postemplacement subsidence of the Hawaiian Ridge. The debris field has a slope of ~1 degree from its center to the edge nearest the outer bench; this value seems reasonable for islandward tilting of the seafloor due to subsidence.

[20] The debris field is partially covered on its southwest half by the Southwest O‘ahu Volcanic Field, first identified in GLORIA imagery (the “West Kaiwi Volcanic Field” of *Holcomb and Robinson* [2004]). The volcanic features were studied in detail during 2001 and 2002 JAMSTEC cruises [*Takahashi et al.*, 2001, 2002]. The field consists of numerous cones and lava flows, clearly defined by bright backscatter on side scan images [*Groome et al.*, 1997]; the cones are also visible in bathymetric data (Figure 2b). The presence of the lavas in side scan sonar imagery indicates that the volcanism, dated by K-Ar at ~3 Ma [*Noguchi and Nakagawa*, 2003], postdated emplacement of the debris field.

3.2.3. Upper Northwestern Block

[21] The northwestern portion of the slump complex is defined by a large block, nearly 40 km in length, that appears to sit atop the main body of the slump (Figure 2a). This block has a well-defined inward-facing scarp, 600 to 700 m-high. The upper edge of the block is wedge-shaped, and has a form similar to the ancient Wai‘anae coastline that lies upslope, from which it is separated by a wide trough. The outer flank of the block slopes gently to the southwest.

3.2.4. Sedimentary Basins and Channels

[22] Several basins are present upon the slump complex, collecting sediments presumably derived from erosion of the subaerial edifice (Figure 2a). The central basin lies at a uniform depth of 2960 m. The trough behind the upper northwestern block reaches 2600 m water depth. Several smaller, elongate basins lie above the southeastern portion of the slump, defining a series of terraces that step

Table 1. Submersible and ROV Dives

Dive[a]	Location Description	Start Point	End Point	Start Depth, m	End Depth, m	Rock[b]	Sediment[b]
		Wai'anae Slump Complex					
K205	toe of central outer bench	21.0552°N, 158.6330°W	21.0630°N, 158.6227°W	4655	4316	27	2
S707	ridge on southeastern portion of outer bench	20.7268°N, 158.1972°W	20.7422°N, 158.1824°W	4342	3940	7	1
T326	inner scarp of upper NW block	21.3911°N, 158.4670°W	21.3841°N, 158.4699°W	2449	1930	31	1
S703	debris field/SW O'ahu Volcanic Field	20.7243°N, 159.2201°W	20.7088°N, 159.2165°W	4525	4478	13	2
		Northwest of Wai'anae					
T325	crest of Ka'ena Ridge	21.7348°N, 158.6236°W	21.7316°N, 158.6287°W	715	653	16	2
T327	basin north of Ka'ena Ridge	21.9352°N, 158.2401°W	21.9215°N, 158.2539°W	3381	3388	1	5
T328	basin north of Ka'ena Ridge	21.9563°N, 158.2182°W	21.9348°N, 158.2404°W	3384	3384	1	

[a] Prefixes indicate *Tiburon* (T), *Kaiko* (K), or *Shinkai 6500* (S) dives.
[b] Number of samples.

down in the seaward direction (the terraced south flank; Figure 2a).

[23] The central basin is cut by a meandering canyon, 500 to 1000 m wide and approximately 100 m deep. The canyon drops over the outer bench just to the south of the bench's more chaotic northern portion. A small sediment fan is visible where the canyon feeds through a narrow slot formed by blocks from the northern slide and outer bench. Channels lead from the basin over the outer face of the slump.

3.2.5. Upper Slope

[24] Above the sediment filled mid-slope basins, the upper slope is covered predominantly by conical talus aprons derived from erosion of the subaerial edifice over a 3 m.y. span. Debris lobes cover the slope both above and below the ancient shoreline (slope break at 1400 m water depth), and some debris lobes drape over this slope break. Detailed side scan imagery over a portion of the upper slope reveals channels of high reflectivity, thought to be talus/debris lobes [*Fornari and Campbell*, 1987]; some debris fingers are large enough to be detected in the bathymetric data (Figure 2a).

4. Dive Observations and Sample Descriptions

[25] Dives conducted in 2001 and 2002 have provided the first seafloor observations and samples of the deep submarine flanks of Wai'anae Volcano and the surrounding area (Figure 1; Table 1). In 2001, MBARI ROV *Tiburon* dives investigated the upper northwestern block (dive T326), the crest of Ka'ena Ridge (T325), and a sediment-filled basin on Wai'anae's north flank (T327 and T328). Two JAMSTEC dives ascended the outer scarp of the outer bench (ROV *Kaiko* dive K205 in 2001 and manned submersible *Shinkai 6500* dive S707 in 2002). Additionally, *Shinkai 6500* dive S703, conducted in 2002 to investigate lava flows from Southwest O'ahu Volcanic Field, encountered the distal extent of the debris field southwest of the outer bench.

[26] Dive site selection in the area was limited by several telecommunication cables that drape the seafloor as they fan out from the O'ahu coast. Rock sampling by ROV and submersible proved difficult in this region because of thick (up to 6 mm) Mn-Fe coating on most of the outcrops, which effectively indurates the rock [e.g., *Moore and Clague*, 2004]. This necessitated some sampling of loose talus, though samples were collected directly from outcrop whenever possible. Bottom sediment was sampled by push core. Locations and descriptions of all samples are given in Appendix A. In Appendix A and the discussion that follows, we classify volcaniclastic rocks according to the scheme of *Clague et al.* [2002], into monomict and polymict breccias and hyaloclastites. Visual records of the seafloor are a

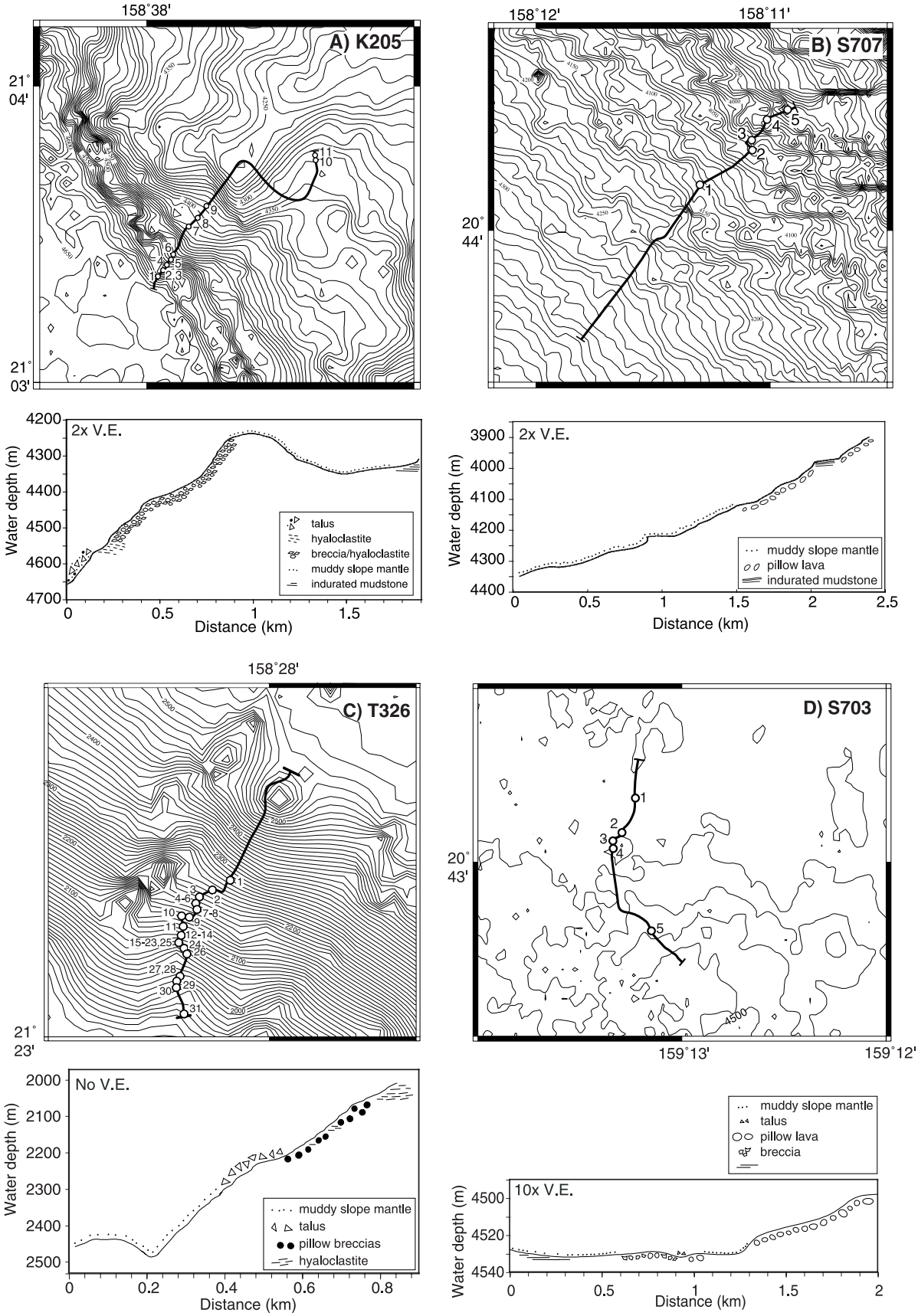
158°38'
A) K205
21° 04'
21° 03'
158°12'
158°11'
B) S707
20° 44'
2x V.E.
Water depth (m)
Distance (km)
talus
hyaloclastite
breccia/hyaloclastite
muddy slope mantle
indurated mudstone
2x V.E.
muddy slope mantle
pillow lava
indurated mudstone
158°28'
C) T326
21° 23'
D) S703
20° 43'
159°13'
159°12'
No V.E.
muddy slope mantle
talus
pillow breccias
hyaloclastite
muddy slope mantle
talus
pillow lava
breccia
10x V.E.

Figure 3

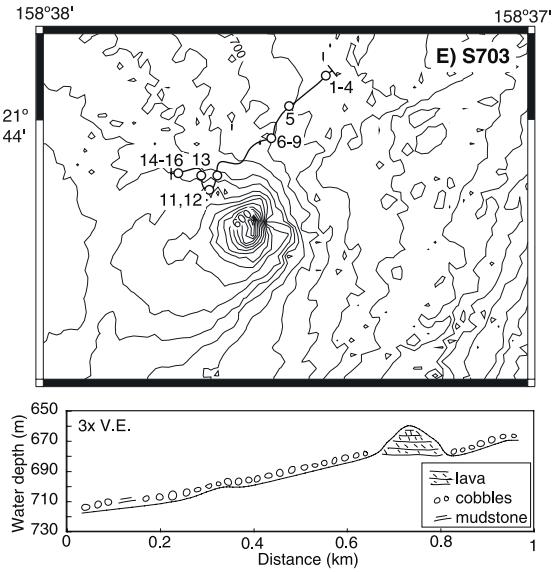

Figure 3. (continued)

combination of video and still film and digital photographs.

4.1. Wai'anae Slump Complex

4.1.1. Dive K205

[27] Dive K205 ascended a steep slope (~21°) near the base of one of the distal ridges low on the central outer bench of the Wai'anae slump complex (Figures 2a and 3a). The first 80 m of elevation gain encountered mud- and sand-covered slopes with increasing amounts of blocks, some grouped to form vague outcrop-like areas. This talus field is not cemented by Mn oxide coating, as evidenced by ease of sampling. Some talus lobes contained angular blocks and have little or no sediment cover. Eight samples of volcanic breccia to mudstone were sampled at four locations during this portion of the dive.

[28] From 4543 m to about 4300 m, jointed and fractured outcrop alternated with talus. The lowermost unit encountered in this sequence of outcrop is ~20 m of bedded, fine-grained hyaloclastite, dipping gently into the slope (Figure 4a). This fine-grained sequence is overlain by coarser breccias (Figure 4b). Breccias are composed of finer-grained, lithified volcaniclastic clasts, not lava fragments, indicating a complex history of sedimentation, diagenesis, and deformation. The rock outcrop on this main portion of the ridge face is highly fractured and has sloughed recently, as evidenced by nearly sediment-free talus at the base of steep outcrops.

[29] Above 4300 m, slope-mantling sediment again predominated. As the slope decreased toward the top of the dive, MnO coating may have increased in thickness, as rocks became strongly cemented. In places, the slope mantling sediment itself was indurated, and veneered with ~2 mm of Mn-Fe oxide, suggesting that little erosion (or sedimentation) was occurring. At the top of the 400-m-high ridge, two small outcrops of mudstone contained clasts of lithified volcanic breccia (sample sites 10 and 11).

[30] Twenty-four lithified samples were collected during K205, all volcaniclastic. Fourteen are polymict breccias containing clasts up to 5 cm in diameter. They are composed of glass (some completely altered to palagonite), crystal fragments, and crystalline flow-interior fragments (Figure 5a). Eight samples are polymict hyaloclastites, distinguished from the above breccias by smaller grain size and a higher proportion of glass to crystalline fragments (Figure 5b). Two samples are monomict hyaloclastites, in which clasts are glass fragments of uniform composition with subordinate crystal fragments. Sample type did not differ systematically with position on the ridge. All samples recovered during K205 are olivine-rich, both as phenocrysts within clasts and as individual olivine crystals in matrix (Figures 5a and 5b).

[31] Cement in breccias and hyaloclastites from this dive can be grouped into two categories. In several samples, grains are cemented by rinds of gel palagonite, with interstices filled by zeolites, predominantly phillipsite as determined by reconnaissance EPMA (Figure 5a). This type of alteration is similar to that described for the deepest drillcore samples within the Hawai'i Scientific Drilling Project hole [*Walton and Schiffman*, 2003]. Other breccias and hyaloclastites are almost completely cemented with palagonite, and minor smectite; zeolites may be present in fractures (Figure 5b).

4.1.2. Dive S707

[32] Dive S707 investigated the southernmost extent of the outer bench (Figure 2). This section of the bench is marked by a series of steep ridges that front

Figure 3. Bathymetry and depth-distance profiles of selected dives, with general lithologic sequences along profiles. Data gridded at 50 m spacing, except for T325, which was gridded at 25 m. Aligned highs parallel to dive track for T326 map are probably artifacts from data merging. Contour intervals, 10 m.

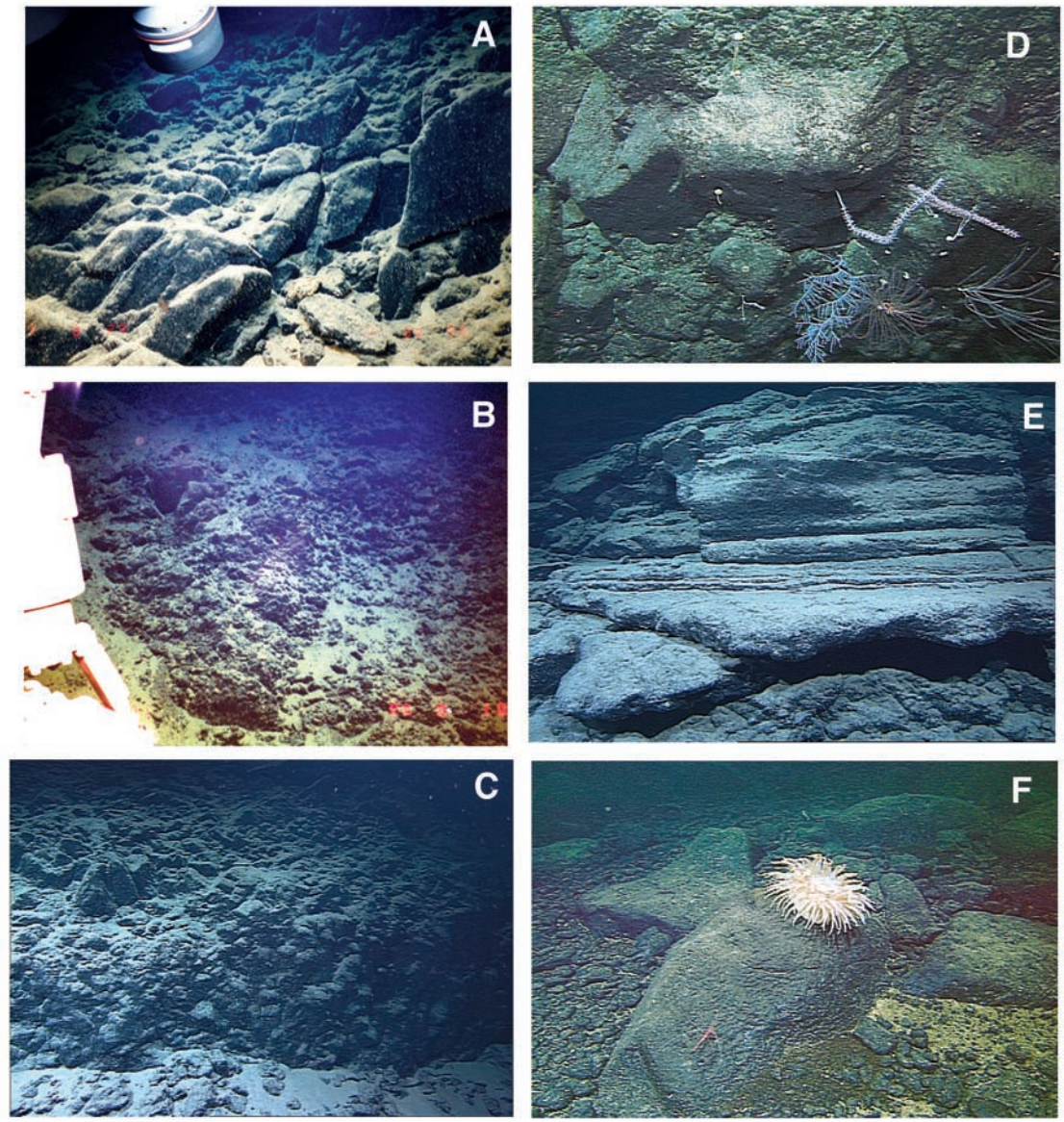

Figure 4. Characteristic volcaniclastic rock types encountered during Wai'anae slump and Ka'ena Ridge dives. (a) Fractured, jointed hyaloclastite from dive K205, 4560 m. Sample K205-5 taken here. (b) Massive, fractured breccia, with clasts of lithified hyaloclastite to fine-grained breccias, from K205. Near site of sample K205-6; 4543 m depth. (c) Massive pillow breccia outcrop, dive T326; 2220 m depth. Sample T326-R6 taken here. (d) Poorly sorted, massive breccia. Dive T326, 1975 m depth. (e) Well-bedded, fine-grained hyaloclastite. Dive T326, 2114 m depth. (f) Rounded cobbles near the top of shield atop Ka'ena Ridge. Dive T325, 713 m depth.

sediment-covered terraces. Dive S707 ascended the third ridge from the base, which has a slope of 15–20 degrees (Figure 3b). The lower slope was completely covered by a blanket of sediment to approximately 4060 m depth. Above a break in slope, the slope is composed of both truncated and intact pillow lavas elongate downslope, in places interbedded with sheet flows and mudstones. A thick section of layered basalt flows was observed at the top of the steep slope as the dive ended, but not sampled due to time restrictions. The relatively intact pillows observed during the dive suggest that if the ridge slumped downslope, it did so as a coherent block with little internal fracturing or deformation.

[33] Seven samples at five locations were collected during S707. All but one (S707-R4) were olivine-phyric basalt pillow fragments, containing 10–15 modal% olivine. All basalt samples are dense

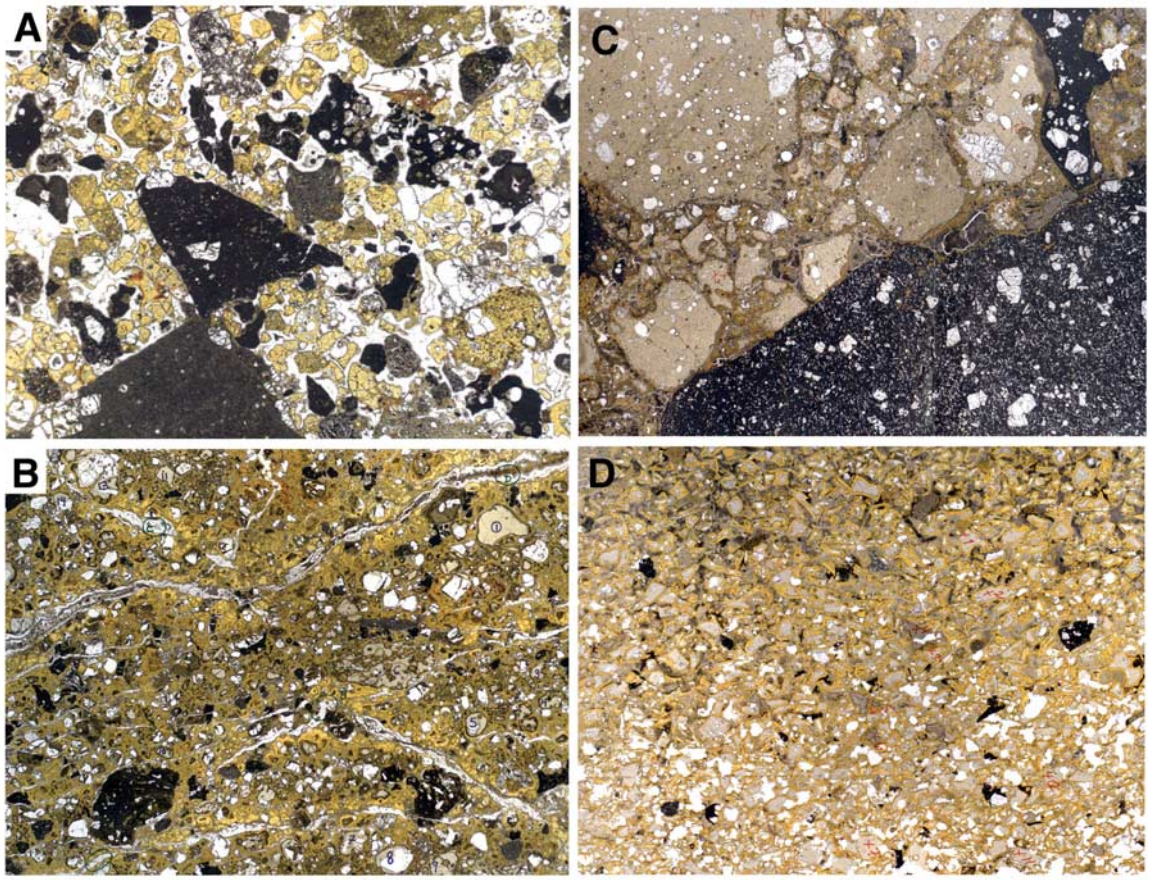

Figure 5. Transmitted light photomicrographs of representative volcaniclastic rocks. (a) Sample K205-2. Lithified polymict breccia. Glass grains have been completely altered to palagonite (yellow) and zeolites (clear areas surrounding grains) fill the interstices. Field of view is 1.6 cm across. (b) Sample K205-3A3. Polymict hyaloclastite with palagonitized matrix. Field of view is 1.9 cm across. (c) Sample T326-R17. Polymict breccia with palagonite-smectite matrix. Fractures are filled with zeolites. Field of view is 2.4 cm across. (d) Sample T326-R30. Fine-grained monomict hyaloclastite with palagonitized glass grains and variable in-filling of void spaces with smectite. Field of view is 1.7 cm across.

(<1% vesicularity) and have MnO rinds up to 6.5 mm thick. Many have indurated mud between basalt and MnO coating. Three (S707-R2a, S707-R3, and S707-R5) have glassy rinds. Sample S707-R4 is a well-indurated, Mn-coated mudstone collected from slope-mantle.

4.1.3. Dive T326

[34] Dive T326 ascended the steep (~25°C), 700-m-high, landward facing scarp of the upper northwestern block (Figures 2 and 3c). Near the base of the scarp, the dive ascended Mn-coated and cemented talus, until the first sample was collected at 2313 m water depth. From this site upward, nearly continuous outcrop consisted mainly of coarse, pillow-fragment breccias, cropping out in stairstep fashion with short cliffs interspersed with narrow ledges (Figure 4c). Breccia clasts range in size from <1 cm to >1 m (Figure 4d). Interspersed within the breccias were finer-grained, well-bedded units; these became more common higher within the block as the dive progressed (Figure 4e). Outcrops and talus for all of dive T326 were heavily coated with Mn oxides, suggesting that material on the slope has moved little since shortly after block emplacement.

[35] Thirty-one samples were collected during T326, and most are breccias containing variably vesicular, olivine-phyric lava clasts with a fine-grained glass-rich matrix (Figure 5c). We interpret the clasts to be pillow fragments and not subaerial lavas due to their holocrystalline interiors, glassy margins, and lack of oxidation. Four samples near the top of the dive are fine-grained hyaloclastite, some with fine-scale bedding. Hyaloclastites

have palagonite cement, but retain pore space (Figure 5d). We were unable to sample fine-grained lower units due to Mn coating.

4.1.4. Dive S703

[36] Dive S703 was conducted to investigate a sheet flow, highly reflective in side scan sonar, in the western part of the Southwest O‘ahu Volcanic Field, but the dive track is also within the bounds of the Wai‘anae debris field (Figures 1 and 2b). The high back-scatter area is flat and covered with mud except some small mounds a few meters to 20 m high (Figure 3d). Two types of mounds were encountered. The first were tumuli of dense, olivine-phyric basalt, 2 to 3 meters high. Manganese oxide coatings on samples collected from tumuli are relatively thin ($\leq$3 mm). Other mounds range in height to 20 m and consist of volcaniclastic material with thick manganese oxide coating (up to 6 mm). The base of one tumulus is underlain by volcaniclastic material, also with thick manganese oxide coating, indicating formation of the tumulus after emplacement of volcaniclastics.

[37] Volcaniclastic rocks were collected at three sites during S703. At the first site a single rounded clast of vesicular basalt was collected. At the second site four clasts were recovered: an olivine-rich monomict hyaloclastite, and three clasts consisting of fragmental but fully crystalline lava, similar to samples from the South Kona Bench offshore of Mauna Loa, and interpreted to be subaerial ‘a‘a lavas [*Yokose and Lipman*, 2004]. Finally, two samples from the base of a 20 m-high mound are glass-rich monomict breccias.

4.2. Northwest of Wai‘anae

4.2.1. Dive T325

[38] Dive T325 investigated a low relief shield volcano atop the central portion of Ka‘ena Ridge (Figure 1). The structure is approximately 7 km across and rises 300–400 m above the surrounding ridge. The dive started on the shield and ascended a satellitic bathymetric high, 750 m in diameter and less than 50 m taller than the surrounding ridge (Figure 3e). It was anticipated that the shield might be a rejuvenated-stage submarine cone; however, observations during the dive indicate that the shield formed subaerially. The dive track initially crossed a series of gravel and cobble beaches (Figure 4f), then encountered massive ‘a‘a flows.

[39] Sixteen rock samples and one sediment push-core were collected. All but two of the rock samples are basaltic lava or lava cobbles. The exceptions are T325-R4, a semi-indurated slope mantling mudstone, and T325-R5, a piece of detrital carbonate. All lavas are aphanitic basalts; most are oxidized.

4.2.2. Dives T327 and T328

[40] The primary purpose of dives T327 and T328 was to measure heat flow in a sediment-filled basin north of Ka‘ena Ridge [*Jordahl et al.*, 2001] (Figure 1). Several samples were also collected, yielding both solid rocks and glass fragments embedded within pelagic sediments mantling the slope. Sample T327-R1 is a clast of olivine plagioclase basalt with partially palagonitized glassy margins. Sample T328-R1 is a medium-grained breccia rich in glassy, plagioclase-phyric clasts.

5. Geochemistry

5.1. Glass Compositions

[41] Major element, S, and Cl composition of hyaloclastite and breccia glass grains, pillow lava rinds, and loose glass grains from sediment cores were measured by wavelength-dispersive electron probe microanalysis (EPMA) using a 5-spectrometer JEOL 8900R electron microprobe at the U.S. Geological Survey (USGS) in Menlo Park, CA (Table 2). EPMA used procedures outlined by *Sisson et al.* [2002] and the standards of *Clague et al.* [1995], with the following exception. SiO_2 values were standardized on Hawaiian basaltic glass standard A99, which gives better agreement with other well-characterized standards than the fragment of Juan de Fuca glass standard VG2 currently in use at the USGS.

[42] For three pillow lava samples from dive S707, reported values are averages of 15 spot analyses. For glass grains from K205 and S703 volcaniclastics, reported values are averages of three spots per grain. One to twenty-seven glass grains per sample were analyzed. Totals used here range from 98.1 to 100.6%. For *Tiburon* samples, single analyses were conducted on glass grains, and statistically identical analyses from the same sample were averaged.

[43] All analyzed glasses from the Wai‘anae slump complex and Ka‘ena Ridge are tholeiitic; a few glasses from dives T327 and T328 from north of Ka‘ena Ridge are alkalic (Figure 6). Glasses span a

Table 2 (Representative Sample). Electron Microprobe Analyses of Submarine Wai'anae Region Glasses (The full Table 2 is available in the HTML version of this article at http://www.g-cubed.org)

Sample	SiO_2[a]	TiO_2	Al_2O_3	FeO	MnO	MgO	CaO	Na_2O	K_2O	P_2O_5	S, ppm	Cl, ppm	Total
S707 Pillow Rinds													
S707-2a	51.7	2.55	14.2	10.3	0.15	6.57	10.9	2.32	0.45	0.26	237	210	99.6
S707-3	51.5	2.53	14.2	10.3	0.14	6.48	11.0	2.29	0.44	0.25	253	181	99.3
S707-5	51.7	2.55	14.2	10.3	0.16	6.79	11.0	2.28	0.44	0.25	254	192	99.7
T326 Hyaloclastite Grains													
T326-R01, 1-6	51.2	2.63	14.5	10.7	0.19	6.23	10.5	2.72	0.51	0.28	29	40	99.5
T326-R02, 1-5	51.6	2.98	14.3	10.3	0.16	5.64	9.92	2.74	0.62	0.40	260	112	98.8
T326-R04 1-5	52.3	3.41	14.2	10.6	0.16	5.03	9.21	2.99	0.76	0.50	240	194	99.2
T326-R06 1-5	52.0	2.98	14.3	10.3	0.16	5.73	9.94	2.76	0.62	0.39	289	146	99.3
T326-R07, 1-7	50.9	3.02	13.7	11.3	0.17	6.00	10.8	2.53	0.53	0.33	38	91	99.2
T326-R09, 1-10	51.1	3.02	13.8	11.5	0.17	6.04	10.8	2.53	0.52	0.34	45	83	99.7
T326-R10, 1, 2, 4-7	50.9	2.83	14.7	10.6	0.15	6.28	9.92	2.73	0.58	0.31	21	32	99.0
T326-R10, 3	51.4	2.50	14.2	10.8	0.15	6.52	10.6	2.44	0.41	0.28	82	90	99.4
T326-R11, 1-7	50.9	3.02	13.6	11.2	0.17	6.12	10.6	2.46	0.52	0.34	41	103	99.0
T326-R12B, 1-6	50.4	3.07	14.9	11.4	0.16	6.04	9.30	2.99	0.65	0.35	20	57	99.3
T326-R13, 1-4, 10	50.3	3.12	13.4	12.4	0.21	5.81	10.6	2.55	0.53	0.33	64	100	99.3
T326-R13, 5	51.7	2.53	14.3	10.6	0.16	6.15	10.3	2.66	0.49	0.26	48	30	99.1
T326-R13, 6	50.0	2.97	13.6	11.7	0.20	6.05	10.8	2.38	0.49	0.30	64	60	98.5
T326-R13, 7-9	50.2	3.13	14.5	11.5	0.16	5.95	9.27	2.96	0.66	0.35	19	37	98.7
T326-R14, 1-5	50.3	3.14	13.4	12.5	0.18	5.63	10.6	2.55	0.54	0.33	66	114	99.3
T326-R15, 1-3, 6	51.1	2.73	14.8	10.8	0.16	6.24	9.70	2.78	0.54	0.30	24	30	99.0
T326-R15, 4, 5	50.9	3.10	14.1	10.9	0.16	5.89	9.67	2.80	0.58	0.32	18	35	98.4
T326-R16, 1-9	51.2	2.94	14.5	11.4	0.17	5.96	9.84	2.86	0.56	0.33	17	70	99.7
T326-R17, 1-4, 6, 7	51.3	2.90	14.6	11.1	0.15	6.12	9.82	2.74	0.56	0.32	32	80	99.6
T326-R18, 1-3	51.6	2.98	13.5	11.3	0.17	5.77	10.2	2.63	0.60	0.34	40	83	99.0
T326-R18, 4-5	50.3	3.15	13.5	12.2	0.19	5.84	10.6	2.56	0.52	0.33	106	85	99.3
T326-R19, 1-4	50.3	2.99	15.2	11.4	0.15	5.98	9.36	3.06	0.64	0.35	10	28	99.4
T326-R21, 1-7	50.2	3.32	13.9	11.5	0.16	5.79	10.0	2.78	0.63	0.38	47	96	98.7
T326-R22, 1-8	50.7	3.43	13.9	12.0	0.18	5.73	10.1	2.84	0.64	0.38	50	99	100.0
T326-R23, 1-7	50.6	3.43	14.0	11.8	0.16	5.69	10.2	2.86	0.66	0.37	63	109	99.8
T326-R24, 1-6	50.6	3.55	13.6	12.0	0.16	5.47	10.1	2.83	0.67	0.39	55	95	99.4
T326-R25 2-4	51.3	2.97	14.4	11.3	0.15	5.94	9.90	2.88	0.58	0.34	15	93	99.7
T326-R25 5	51.8	2.76	15.3	11.2	0.13	6.39	10.2	2.95	0.44	0.32	26	70	101.5
T326-R25 6	52.5	3.14	14.8	11.7	0.20	5.65	9.43	2.90	0.39	0.41	0	30	101.1
T326-R26, 1-6	49.4	3.27	13.5	10.9	0.15	5.77	9.69	2.77	0.62	0.38	44	107	96.6
T326-R28, 1-6	51.1	3.31	13.4	11.6	0.18	5.62	10.1	2.54	0.61	0.38	26	103	98.9
T326-R29, 1-9	50.0	2.74	14.4	11.4	0.17	6.54	11.4	2.49	0.45	0.29	43	110	99.8
T326-R30, 1-3, 5, 7-12	50.7	2.62	14.2	10.6	0.18	6.62	10.9	2.37	0.44	0.28	13	54	98.8
T326-R30, 4, 6	50.6	3.26	13.3	11.6	0.17	5.90	10.3	2.48	0.56	0.36	15	120	98.5
T326 Loose Grains From Cores													
T326-PC61G 2	48.8	4.68	15.1	14.1	0.21	5.42	8.62	1.85	0.96	0.72	78	150	100.4
T326-PC61G 3	51.0	2.66	13.8	11.4	0.19	6.24	11.0	2.39	0.46	0.31	29	120	99.5
T326-PC61G 4	52.0	2.68	14.8	10.9	0.20	6.71	9.19	2.78	0.56	0.30	18	30	100.1
T326-PC61G 5	51.1	2.62	14.1	11.3	0.18	6.37	11.0	2.36	0.40	0.27	29	90	99.7
T326-PC61G 6	51.5	2.50	14.7	10.7	0.20	6.36	10.4	2.72	0.48	0.26	46	20	99.8
T326-PC61G 7	51.9	2.30	14.7	10.6	0.21	6.30	10.0	2.76	0.47	0.24	13	20	99.6
T327 Loose Grains From Cores													
T327-PC65G 1	52.7	2.31	14.4	10.3	0.13	5.94	9.99	2.75	0.48	0.30	0	290	99.4
T327-PC65G 2	53.7	2.87	13.8	10.9	0.16	5.03	9.15	3.07	0.86	0.43	0	50	100.0
T327-PC65G 3	54.8	2.99	14.2	10.0	0.18	4.52	8.12	3.17	1.14	0.49	0	60	99.6
T327-PC65G 4	54.5	3.10	14.0	10.2	0.17	4.65	8.34	3.13	1.09	0.55	0	50	99.8
T327-PC65G 5	51.6	2.61	14.3	10.5	0.17	6.76	10.6	2.41	0.37	0.23	10	50	99.5
T327-PC65G 6	53.4	2.01	14.6	10.4	0.15	6.10	10.0	2.56	0.40	0.23	3	0	99.9
T327-PC65G 7	51.6	2.46	14.3	10.4	0.22	6.49	10.6	2.45	0.38	0.26	26	130	99.2
T327-PC76G 1	53.6	2.44	14.2	10.3	0.17	5.57	9.69	2.84	0.62	0.37	18	60	99.7
T327-PC76G 2	52.8	2.38	14.1	10.1	0.16	5.71	9.80	2.70	0.62	0.35	10	70	98.8
T327-PC76G 3	53.5	3.01	14.7	9.7	0.10	5.18	8.70	3.28	0.96	0.45	32	70	99.5
T327-PC76G 4	54.7	3.06	14.0	10.4	0.13	4.56	8.21	3.12	1.12	0.56	27	120	99.9

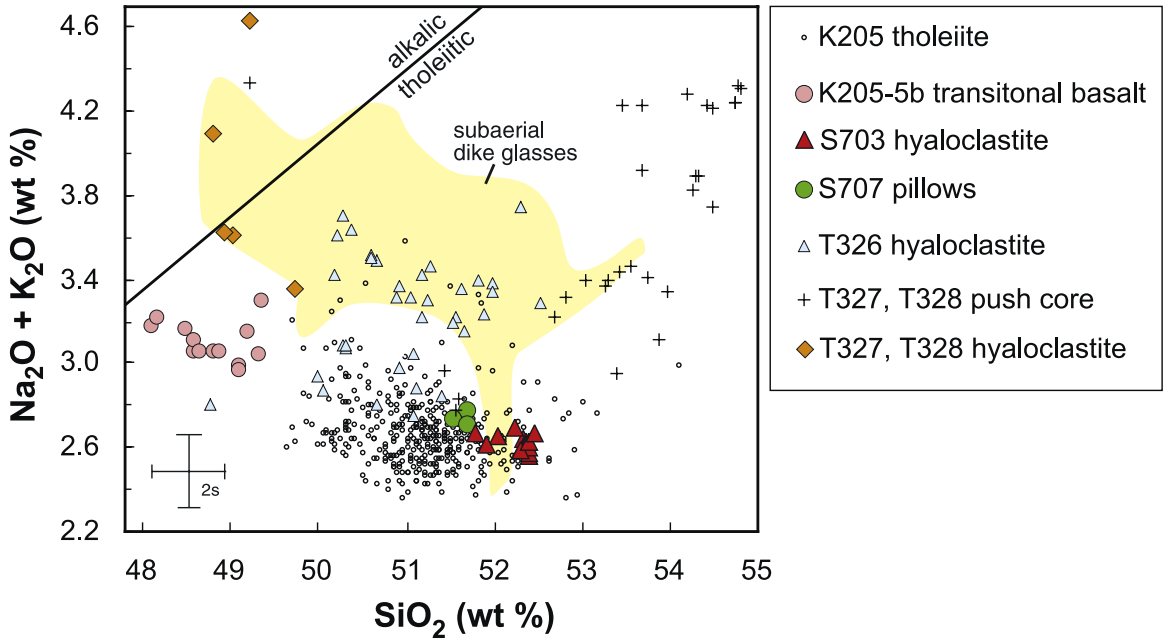

Figure 6. Total alkali-silica diagram for submarine glass from the Wai'anae region. Glasses from dikes of the subaerial edifice of Wai'anae Volcano, correlating primarily to lavas of the Kamaile'unu Member of the Wai'anae Volcanics, taken from *Zbinden and Sinton* [1988] and shown in yellow field. Alkalic-tholeiitic boundary from *Macdonald and Katsura* [1964].

large compositional range, however, in terms of SiO_2, MgO, alkalis, and other incompatible elements, and many form distinct fields on variation diagrams.

[44] The glasses from outer bench dive K205 are all grains within breccias or hyaloclastites or glassy portions of partially crystalline clasts and can be broken into two subgroups on the basis of composition. Glass grains from all but one sample fall well within the tholeiitic field on a silica-total alkalis variation diagram (Figure 6). These tholeiites range in SiO_2 from 49.6 to 53.1 wt% (a single analyzed grain has 54.1 wt% SiO_2), and in MgO from 8.6 to 5.5 wt% (Figure 7). All but five tholeiite grains are degassed, with S contents <300 ppm, suggesting subaerial eruption. The remaining five have S between 300 and 800 ppm; these lie at the high-MgO within this group (Figure 7). A much smaller suite of glass grains, all from a single sample (K205-5b), is compositionally distinct from the tholeiite glasses described above (Figures 6 and 7). These grains have lower SiO_2 (48.2 to 49.3 wt%), and are generally more fractionated than the tholeiite group (5.6 to 6.3 wt% MgO). In addition, they have higher S contents (220 to 520 ppm). They lie within the tholeiite field on a total alkalis versus silica diagram, but are close to the alkalic-tholeiitic boundary as defined by *Macdonald and Katsura* [1964]. Thus they are "transitional" according to the convention adopted by *Wolfe et al.* [1997] for Mauna Kea basalts and *Sisson et al.* [2002] for samples from the submarine south flank of Kīlauea.

[45] The three pillow rinds from the south outer bench (S707) are compositionally identical within analytical error and fall in the middle of the tholeiite group of glasses from K205 on all variation diagrams (Figures 6–8). All three lavas are degassed (<300 ppm S, 0.1 wt% H_2O, and CO_2 below detection as determined by infrared spectroscopy), suggesting that they originally erupted subaerially and then crossed the shoreline.

[46] A single hyaloclastite from dive S703 on the deep seafloor debris field contains tholeiitic glass grains that fall within compositional fields of outer bench glasses (Figures 6 and 7). The glass grains are uniformly low in S (Figure 7).

[47] Glasses from T326, on the upper northwestern block, include glass grains in matrix adhering to larger, crystalline basalt clasts, glassy margins on pillow fragments from breccia, and finer grains of glass within hyaloclastite. There are no systematic differences in composition between these different groups of glass from T326. The T326 glasses exhibit a range in SiO_2 similar to K205 tholeiites (48.8 to 52.5 wt%) but are distinctly higher in

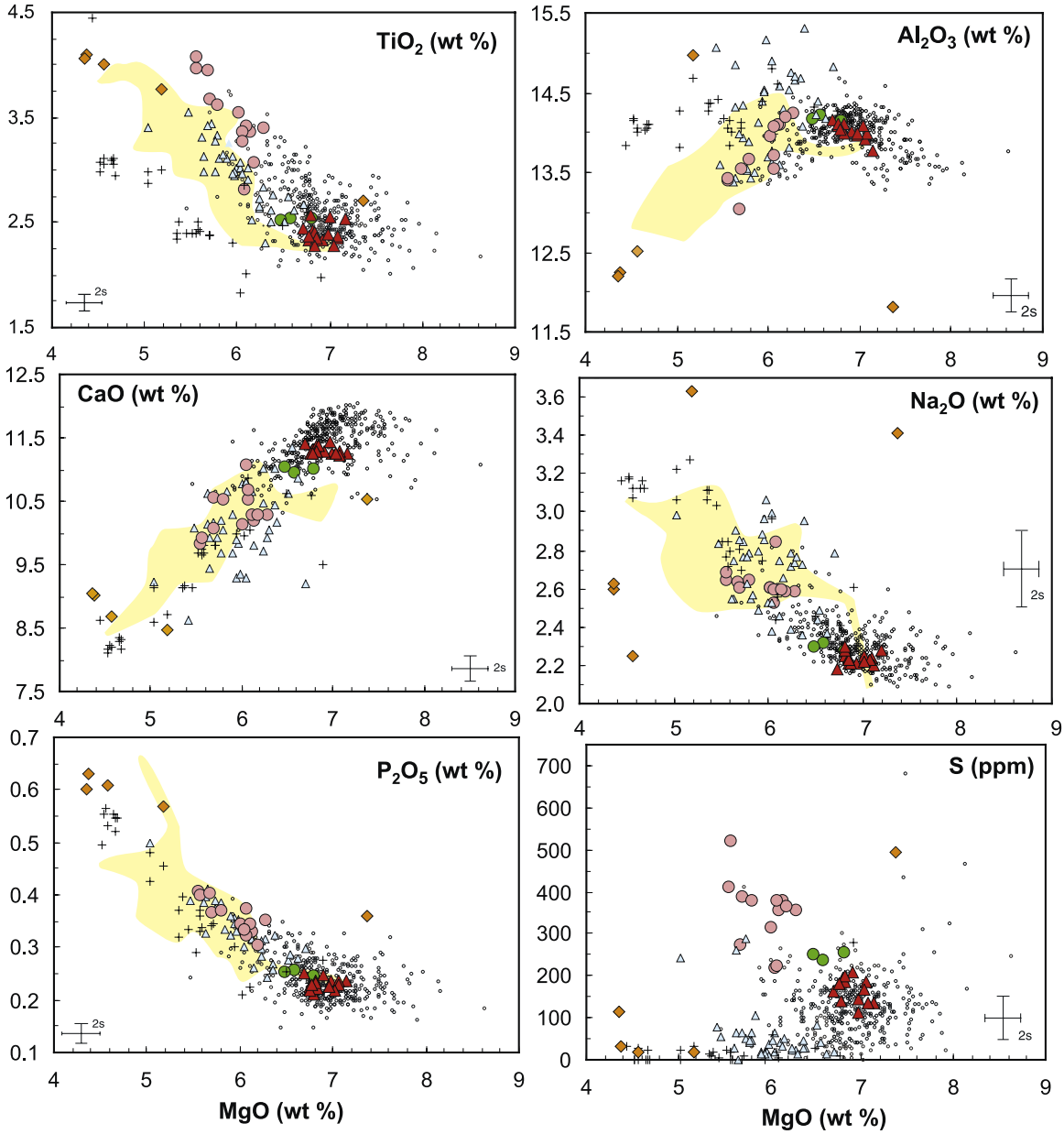

Figure 7. MgO variations diagrams for glasses recovered from the Wai'anae region. Data sources and symbols as in Figure 6.

alkalis (2.7 to 3.8 wt% $Na_2O + K_2O$) and are in general more fractionated (5.5 to 6.7 wt% MgO; Figures 6 and 7). In addition, they have even lower S contents (all but three glasses have S < 100 ppm). Though they plot similarly to the K205-5b transitional glasses on some variation diagrams (Figure 7), they are higher in SiO_2 and Al_2O_3 and slightly lower in TiO_2.

[48] Glasses from dives T327 and T328, both north of Ka'ena Ridge, show the greatest compositional diversity of all the samples analyzed during this study. Glass grains found within push cores and glass grains from hyaloclastite are shown in Figures 6–8. With the exception of a single glass grain of alkali basalt, glasses from the push cores are tholeiites, many of them with high SiO_2; all but three have between 52.7 and 54.8 wt% SiO_2 (Figure 6). At a given MgO, the high-SiO_2 glasses have elevated alkalis and lower TiO_2 relative to glasses collected during the Wai'anae slump dives (Figure 7). All have S less than 300 ppm; all but one have S less than 100 ppm. These glasses are compositionally similar to glasses attributed to

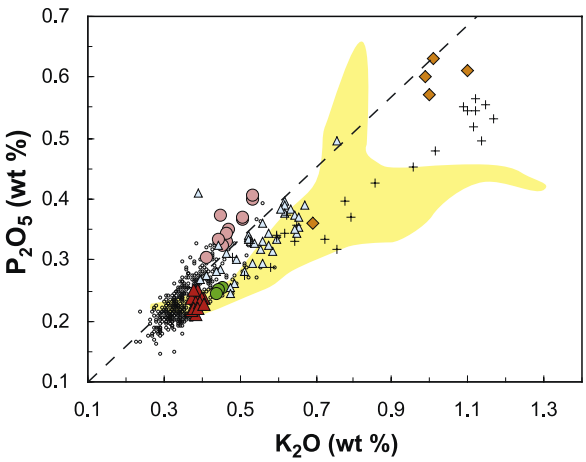

Figure 8. K_2O versus P_2O_5 (wt %) for glasses from the Wai‘anae region. Data sources and symbols as in Figure 6. Dashed line shows reference K_2O/P_2O_5 ratio of 1.67 [*Wright*, 1971].

Ko‘olau volcano [*Sherman et al.*, 2002]. Five glass grains from hyaloclastite samples collected from dives T327 and T328 have SiO_2 between 48.8 and 49.7 wt%, and trend from transitional to alkali basalt (Figures 6 and 7). Other than Na_2O, these five grains most resemble Wai‘anae dike glasses (see below).

[49] For comparison, we have included the only published glass data from subaerial Wai‘anae Volcano on our variation diagrams. *Zbinden and Sinton* [1988] analyzed quenched glassy margins of dikes primarily within the eroded caldera but including several samples from the volcano’s northwest rift zone. The samples are interpreted to be from the late phase of Wai‘anae’s shield stage, corresponding to Kamaile‘unu Member lavas. They are generally tholeiitic, but more fractionated than the tholeiites from the slump’s outer bench (Figure 7). They overlap with glasses from T326 on most variation diagrams (Figures 6 and 7).

[50] K_2O/P_2O_5 ratios are thought to remain relatively constant over a wide range of Hawaiian glasses and fresh lavas [*Clague et al.*, 1995; *Frey et al.*, 2000; *Sisson et al.*, 2002], and for this reason low ratios have been used to identify altered rocks [*Garcia et al.*, 1989; *Lipman et al.*, 1990; *Frey et al.*, 1994]. Values between 1.5 and 2.0 are thought to be indicative of fresh glasses and lavas [*Sherman et al.*, 2002], whereas values below 1.5 are assumed to have lost K_2O during alteration. Values of 1.62 to 1.67 have been suggested as normal for a wide range of compositions [*Wright*, 1971], although preshield alkalic lavas from Kīlauea range to ratios of ~3 [*Sisson et al.*, 2002]. Analyzed glasses from this study exhibit a relatively wide range in K_2O/P_2O_5 ratios, from ~1.2 to ~2.0, and form a fan-shaped array on a P_2O_5-K_2O variation diagram (Figure 8). Transitional basalts from sample K205-5b have an average K_2O/P_2O_5 ratio of 1.34, and fall at one edge of this array. Instead of suggesting alteration and K-loss, however, we propose that the transitional basalts and tholeiites with low ratios instead have high P_2O_5. If postmagmatic alteration had lowered the K_2O in the transitional basalts, one would not expect the linear array that is seen in Figure 8. Therefore the array of K_2O/P_2O_5 ratios for the Wai‘anae glasses is probably real, and glasses from this volcano have magmatic values that are lower than previously recorded for other Hawaiian centers.

5.2. Whole Rock Compositions

[51] Major and trace element whole rock analyses were conducted on six lava and cobble samples from dive T325, seventeen breccia clasts from dive T326, a single breccia clast from T327, and four pillow lavas from S707 (Table 3). Samples were trimmed to remove visible weathering rinds, ground to remove saw marks, and then washed in deionized water in an ultrasonic bath. Rock chips of T325 samples, which were highly altered and contained secondary carbonate, were also washed in a weak acid prior to crushing. Analyses were conducted at Washington State University, using XRF for major elements plus Ni, Cr, V, Y, Ga, Cu, and Zn and ICPMS for remaining trace elements.

[52] All analyzed samples are tholeiitic basalts ranging in MgO from ~6 to ~15 wt% MgO, and in general have elemental abundances that overlap with shield-building tholeiites from other Hawaiian volcanoes (Figure 9). All samples show similar chondrite-normalized REE patterns, with gently sloping light REEs and more steeply sloping heavy REEs (Figure 10a). Trace element spider diagram variations, normalized to NMORB, show a greater variation among the samples, especially within the Ka‘ena Ridge samples (T325; Figure 10b).

[53] In the following discussion, we compare submarine-collected samples to those from the volcano’s subaerial edifice, using MgO variation diagrams and trace element ratios (Figures 9 and 11). Subaerial lavas [*Guillou et al.*, 2000; J. Sinton, unpublished data] are from the Lualualei and Kamaile‘unu Members of the Wai‘anae

Table 3 (Representative Sample). Major and Trace Element Concentrations (The full Table 3 is available in the HTML version of this article at http://www.g-cubed.org)

	Sample													
	S707-R1	S707-R2	S707-R3	S707-R5	T326-R1	T326-R2	T326-R4	T326-R5	T326-R6	T326-R7	T326-R8	T326-R9	T326-R10	T326-R11
Type	pillow lava	pillow lava	pillow lava	pillow lava	breccia clast	breccia clast	breccia clast	breccia clast	breccia clast	breccia clast	breccia clast	breccia clast	breccia clast	breccia clast
Depth, m	4057	4009	3977	3940	2315	2293	2267	2235	2220	2178	2153	2143	2134	2125
SiO_2, wt%	48.35	48.53	48.89	48.70	50.27	49.62	51.52	48.71	47.91	50.31	50.49	50.90	50.16	49.90
TiO_2	1.991	2.042	2.060	1.998	2.71	2.45	3.09	2.53	2.48	2.63	2.65	2.66	2.59	2.59
Al_2O_3	10.93	11.14	11.27	10.91	14.53	11.61	13.08	11.95	11.60	13.39	13.42	13.61	14.38	13.16
FeO	11.37	11.28	11.27	11.29	10.90	11.04	11.02	11.54	11.75	10.71	10.66	10.68	10.17	10.93
MnO	0.168	0.166	0.168	0.169	0.14	0.16	0.15	0.16	0.15	0.16	0.17	0.17	0.14	0.16
MgO	8.82	8.95	9.07	8.79	8.53	13.62	8.04	13.04	13.86	9.13	8.65	8.56	8.75	9.12
CaO	15.09	14.67	14.36	15.17	8.94	8.19	8.58	8.55	8.39	10.51	10.58	10.57	9.74	10.45
Na_2O	0.36	0.36	0.36	0.35	2.81	2.22	2.68	2.24	2.21	2.34	2.39	2.37	2.75	2.35
K_2O	1.79	1.98	1.89	1.84	0.65	0.55	0.78	0.53	0.54	0.46	0.52	0.48	0.58	0.51
P_2O_5	0.207	0.209	0.210	0.205	0.32	0.32	0.41	0.34	0.35	0.29	0.31	0.30	0.31	0.32
Total	99.07	99.33	99.55	99.42	99.80	99.78	99.35	99.58	99.24	99.94	99.83	100.30	99.56	99.50
Ni, ppm	609	583	548	616	219	527	193	464	522	187	173	163	194	212
Cr	804	795	785	801	272	709	309	656	702	447	404	397	349	458
V	253	254	247	246	257	277	335	291	291	307	314	312	299	307
Y	22	21	22	21	27	31	38	33	30	29	28	28	27	27
Ga	16	17	16	18	22	17	21	16	19	21	19	17	20	20
Cu	102	106	105	106	72	82	82	80	76	108	104	107	90	105
Zn	95	98	98	96	112	106	115	115	114	106	106	100	107	104
La	9.50	9.56	9.61	9.18	13.32	13.54	17.23	15.32	14.58	12.60	12.69	12.62	12.59	12.47
Ce	22.00	22.20	22.46	21.78	31.27	31.92	41.09	33.69	32.76	29.60	29.91	29.75	29.18	29.27
Pr	3.27	3.23	3.30	3.17	4.57	4.64	5.91	5.02	4.79	4.33	4.37	4.35	4.24	4.25
Nd	15.45	15.39	15.65	15.16	21.50	21.67	27.27	23.33	22.36	20.34	20.63	20.41	19.88	19.95
Sm	4.38	4.33	4.45	4.35	6.10	6.08	7.69	6.50	6.23	5.79	5.71	5.82	5.55	5.78
Eu	1.47	1.44	1.46	1.44	2.03	1.92	2.43	2.07	1.98	1.91	1.89	1.89	1.89	1.88
Gd	4.60	4.63	4.69	4.52	6.38	6.38	7.91	6.79	6.50	6.15	6.11	6.13	5.85	6.01
Tb	0.72	0.72	0.72	0.70	0.96	0.98	1.23	1.05	1.01	0.94	0.95	0.95	0.90	0.93
Dy	4.15	4.13	4.16	4.01	5.28	5.57	6.98	6.02	5.76	5.40	5.41	5.40	5.14	5.31
Ho	0.78	0.78	0.78	0.76	0.96	1.04	1.30	1.13	1.08	1.00	1.02	1.00	0.97	1.01
Er	2.05	1.97	2.04	1.98	2.42	2.64	3.39	2.94	2.80	2.58	2.55	2.60	2.52	2.55
Tm	0.27	0.27	0.27	0.27	0.32	0.36	0.45	0.40	0.38	0.36	0.35	0.35	0.34	0.35
Yb	1.66	1.62	1.68	1.62	1.89	2.13	2.71	2.37	2.27	2.14	2.12	2.10	1.99	2.11
Lu	0.25	0.25	0.25	0.24	0.28	0.32	0.41	0.36	0.34	0.32	0.32	0.32	0.30	0.32
Ba	60	54	62	62	90	94	130	73	60	110	82	88	76	180
Th	0.50	0.51	0.52	0.51	0.69	0.81	1.09	0.83	0.83	0.73	0.74	0.73	0.66	0.72
Nb	10.01	10.05	10.29	10.01	13.21	15.18	20.47	15.74	15.09	14.53	14.56	14.14	13.06	14.39
Y	22.53	22.40	22.86	21.93	28.30	30.53	37.79	34.74	32.85	29.73	29.63	29.92	29.05	29.64

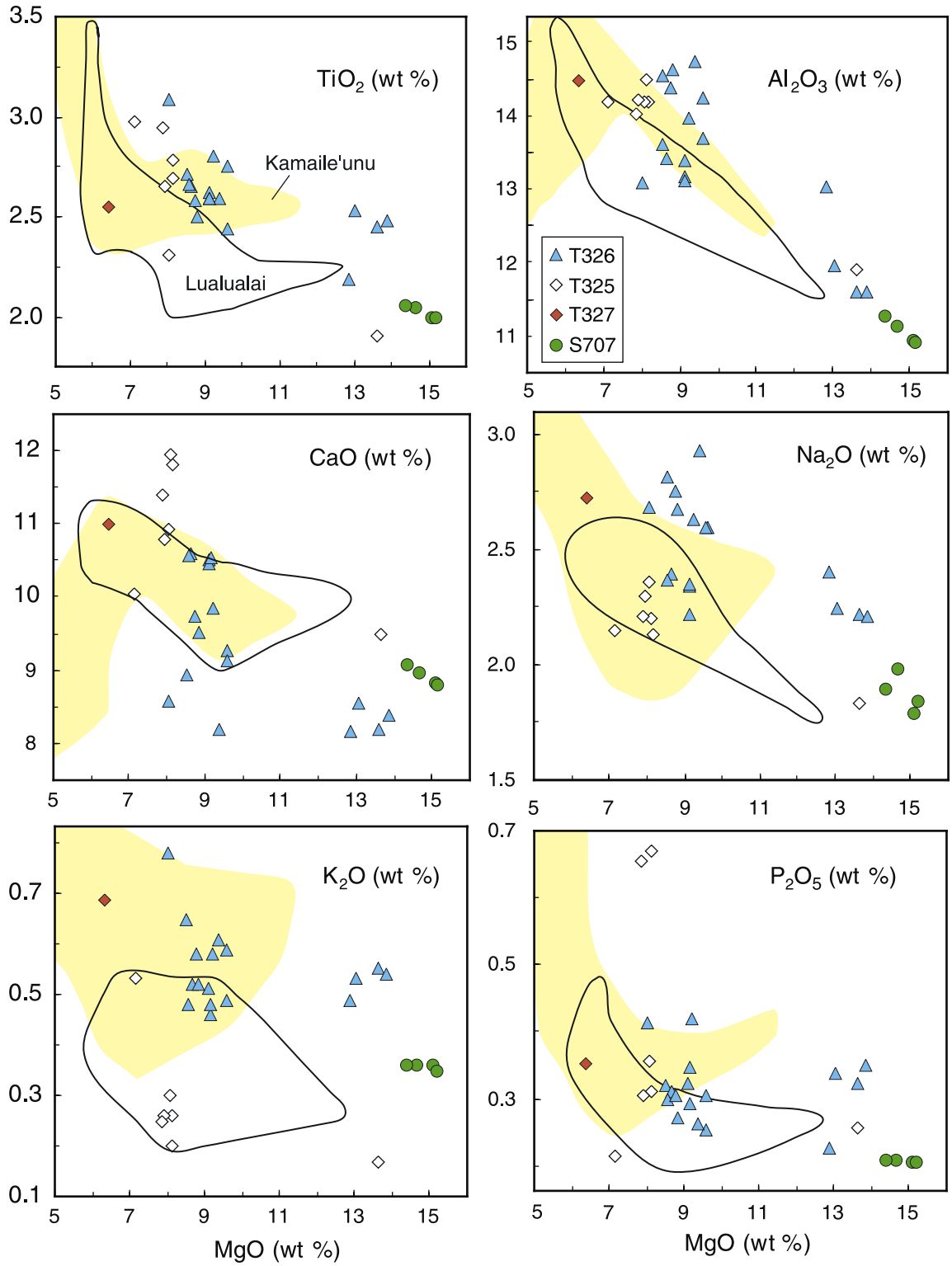

Figure 9. Whole rock MgO variation diagrams for S707 pillow lavas, T326 clasts, T325 lava and clasts, and T327 clast. Fields for shield stage Wai'anae lavas from Lualualei (bounded by solid black line) and Kamaile'unu (in yellow) members [*Guillou et al.*, 2000; J. Sinton, unpublished data] are shown for reference.

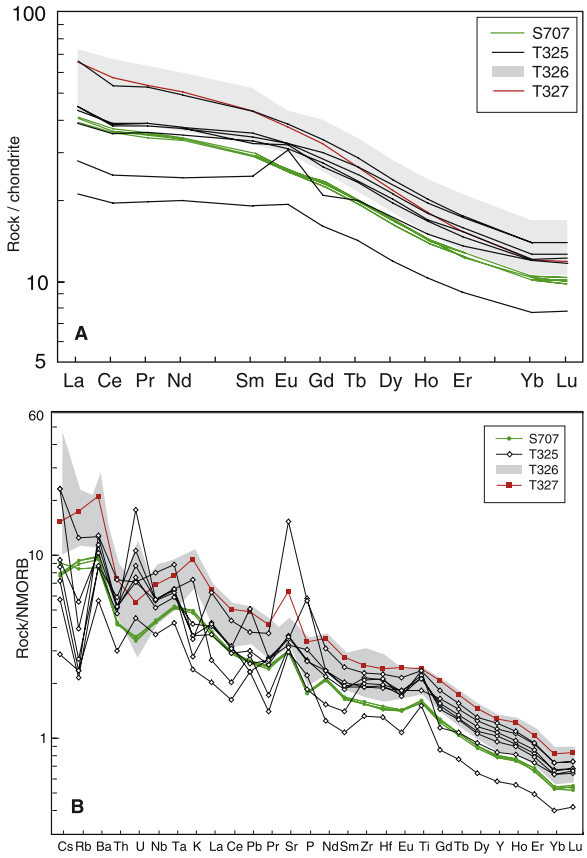

Figure 10. (a) Chondrite-normalized [*McDonough and Sun*, 1995] rare earth element abundances. (b) N-MORB-normalized [*Sun and McDonough*, 1989] incompatible element abundances.

Volcanics, erupted from 3.93 to 3.54 Ma and 3.57 to 3.08 Ma, respectively [*Guillou et al.*, 2000]. These members represent the volcano's early (or main) and late shield stages, and exhibit systematic compositional differences.

[54] In detail, the four lavas from outer bench dive S707 are tightly clustered in variation diagrams and are MgO-rich (14.4 to 15.2 wt%; Figure 9), reflecting their olivine-rich nature. They fall along trends defined by subaerial Lualualei lavas, but at higher MgO contents (Figure 9). They also have similar Ba/Zr and Sr/Nb ratios to Lualualei lavas (Figure 11).

[55] Clasts from the upper block (T326) are tholeiitic and range from 8.0 to 13.9 wt% MgO, and are enriched in incompatible elements relative to S707 lavas for a similar range in MgO. The samples cluster at ~13 wt% MgO and 8–10 wt% MgO, and at a given MgO, there is considerable range in most elements. They span similar ranges to Kamaile'unu lavas in both Ba/Zr and Sr/Nb values (Figure 11), but only partially overlap with Kamaile'unu lavas on MgO variation diagrams (Figure 9).

[56] Lavas from Ka'ena Ridge dive T325 also show considerable scatter in many elements over a small range in MgO, (Figure 9). They have trace element ratios similar to those of S707 lavas (Figure 11). Some element abundances may be affected by alteration in these once-subaerial lavas. In particular, elevated P_2O_5 may be the result of phosphorization and elevated CaO may be from secondary carbonate that was not fully removed by leaching during sample preparation. A single breccia clast from dive T327 exhibits major and trace element abundances that are similar to those of Kamaile'unu lavas.

5.3. Radiogenic Isotopes

[57] With the exception of samples from dive T325, rocks that were analyzed for whole rock chemistry were also analyzed for Sr, Nd, and Pb

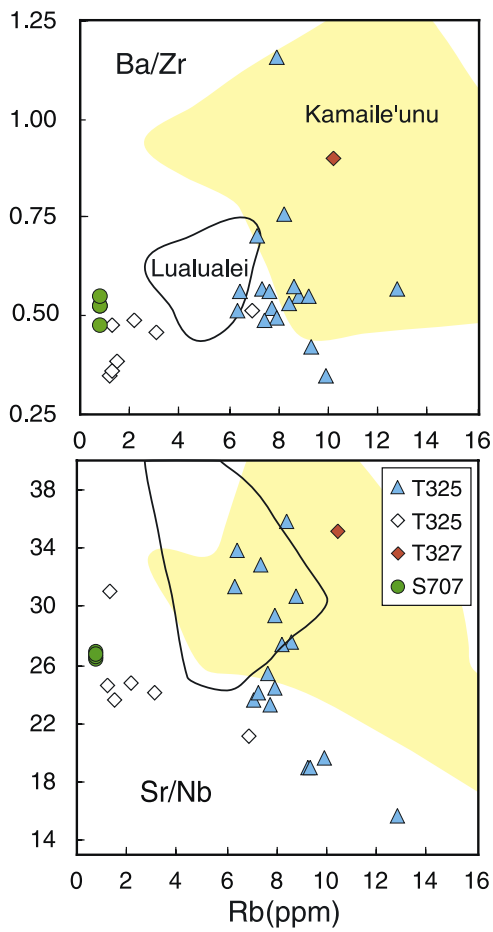

Figure 11. Incompatible element variation diagrams. Data sources and symbols are the same as for Figure 9.

Table 4. Pb, Sr, and Nd Isotopic Compositions

Sample	$^{208}Pb/^{204}Pb$	2σ	$^{207}Pb/^{204}Pb$	2σ	$^{206}Pb/^{204}Pb$	2σ	$^{87}Sr/^{86}Sr$	2σ[a]	$^{143}Nd/^{144}Nd$	2σ[a]
S707-1	37.92	0.057	15.473	0.023	18.157	0.027	0.703706	10	0.512946	12
S707-2	37.809	0.025	15.436	0.01	18.118	0.012	0.703707	9	0.512961	5
S707-3	37.887	0.024	15.468	0.009	18.15	0.011	0.703726	9	0.512944	11
S707-5	37.84	0.028	15.451	0.011	18.134	0.013	0.703743	11	0.512962	10
T326-R1	37.739	0.02	15.434	0.008	17.922	0.01	0.703562	12	0.512936	10
T326-R6	37.838	0.014	15.446	0.006	18.189	0.007	0.703564	12	0.513053	18
T326-R8	37.891	0.005	15.464	0.002	18.218	0.002	0.703558	10	0.513059	6
T326-R11	37.915	0.02	15.473	0.08	18.229	0.01	0.703518	9	0.513042	13
T326-R19	37.887	0.024	15.472	0.01	18.055	0.011	0.7038	10	0.512852	16
T327-R1	37.751	0.016	15.465	0.006	18.043	0.007	0.703721	8	0.512981	19

[a] 2-sigma error, quoting only the fifth and sixth decimal place. All quoted errors are within-run uncertainties only; see text for long-term precision estimates.

isotopic compositions at Carleton University, Ottawa, Ontario (Table 4). Sample powders were acid-washed in hot 1.5N HCl for two hours, rinsed twice in ultrapure H_2O, and then dissolved in HF/HNO_3. Pb, Sr and Nd were extracted sequentially following the procedures outlined by *Cousens* [1996]. Isotope ratios were determined on a Finnigan MAT261 multicollector mass spectrometer running in static mode. Nd isotope ratios are normalized to $^{146}Nd/^{144}Nd = 0.72190$. > 100 runs of the La Jolla standard average $^{143}Nd/^{144}Nd = 0.511876 \pm 18$ (2-sigma, September 1992–December 2003). Sr isotope ratios are normalized to $^{86}Sr/^{88}Sr = 0.11940$ to correct for fractionation. Two Sr standards are run at Carleton, NIST SRM987 ($^{87}Sr/^{86}Sr = 0.710251 \pm 18$, n = 55, September 1992–December 2003) and the Eimer and Amend (E&A) $SrCO_3$ ($^{87}Sr/^{86}Sr = 0.708032 \pm 25$, n = 30, September 1994–December 2003). All Pb mass spectrometer runs are corrected for fractionation using NIST SRM981. The average ratios measured for SRM981 are $^{206}Pb/^{204}Pb = 16.890 \pm 0.012$, $^{207}Pb/^{204}Pb = 15.429 \pm 0.014$, and $^{208}Pb/^{204}Pb = 36.502 \pm 0.048$ (2 sigma), based on >100 runs between September 1992 and December 2003. The fractionation correction is +0.13%/amu (based on accepted values of *Todt et al.* [1984]).

[58] Figure 12 presents the new isotopic data, compared to published data from Ko'olau and Wai'anae Volcanoes. S707 samples are isotopically homogeneous, and fall within the Wai'anae fields for Sr, Nd, and Pb. The lone sample from dive T327 also plots within the Wai'anae fields. Samples from Dive T326 are slightly more variable in composition. Sample T326-R19 has higher $^{87}Sr/^{86}Sr$ and lower $^{143}Nd/^{144}Nd$ ratios compared with previously analyzed Wai'anae lavas, whereas R6, R8 and R11 have higher $^{143}Nd/^{144}Nd$ (Figure 12a). Sample T326-R1 has lower $^{206}Pb/^{204}Pb$ that falls just outside the Wai'anae field.

6. Discussion

6.1. Origins of Wai'anae Slump Material

[59] Hawaiian volcanoes are thought to evolve through three main eruptive stages: a small-volume, alkalic preshield (Lōihi) stage, a voluminous, tholeiitic shield stage, and a small-volume postshield alkalic stage. Finally, after a period of quiescence that varies in duration, a very small-volume alkalic rejuvenated stage may take place [*Stearns*, 1946; *Clague and Dalrymple*, 1987]. Samples representing the preshield phase are rare, and have only been described from Lōihi Seamount [*Moore et al.*, 1982], and now Kīlauea Volcano [*Lipman et al.*, 2002; *Sisson et al.*, 2002]. Our understanding of the shield and postshield stages of Hawaiian volcanoes has come predominantly from studying subaerial exposures, although recent submarine studies have extended these observations.

[60] A volcano's evolution as it passes over the mantle melting anomaly will not only affect the composition of magma that is erupted, but will also play a role in the development of the volcanic edifice. Slumps are a common feature of submarine volcanic flanks in Hawai'i, and are thought to form by intermittent motion, driven by a combination of gravitational instability and lateral forces resulting from injection of magma into a volcano's rift zones [*Moore et al.*, 1989; *Borgia and Treves*, 1992; *Denlinger and Okubo*, 1995]. Such landslides seem most likely to form during the height of shield building, when magma production is highest and the subaerial edifice is largest [*Moore et al.*, 1989]. If slumping generally occurs during mid- to late-

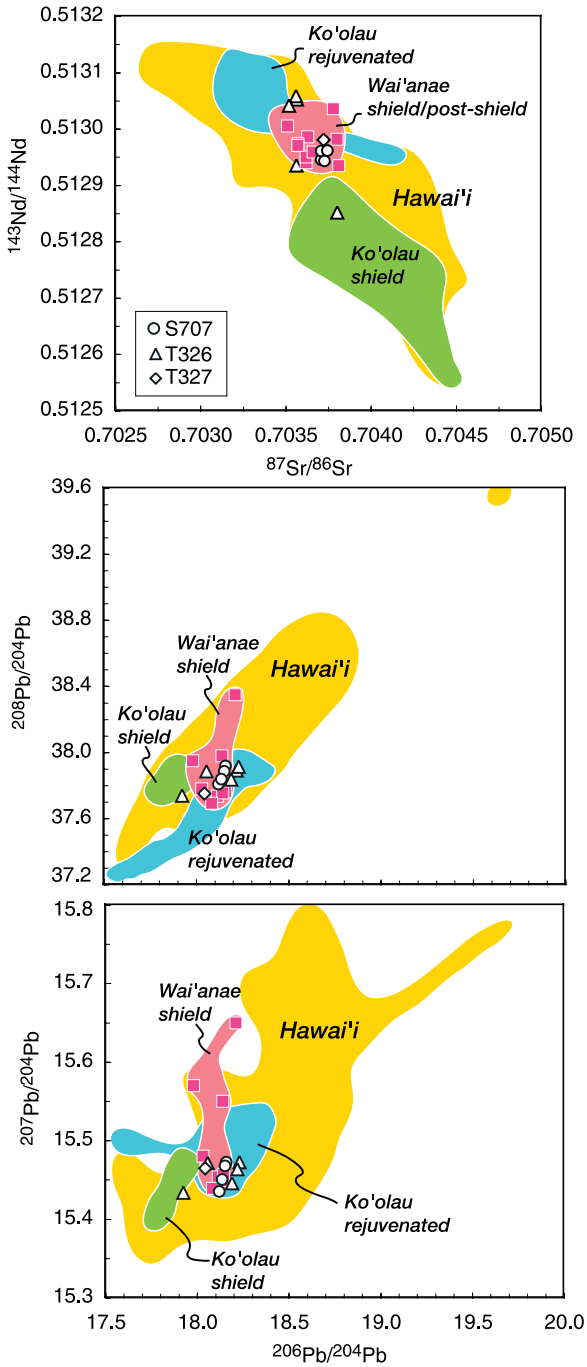

Figure 12. (a) Isotope variation plots for submarine Wai'anae rocks, plotted against fields for previously reported lavas from Wai'anae, Ko'olau, and other Hawaiian volcanoes. Subaerial Wai'anae data from *White and Hoffman* [1982] and *Stille et al.* [1983]. Data for other lavas are from the GEOROC database. (a) $^{143}Nd/^{144}Nd$ versus $^{87}Sr/^{86}Sr$. (b) $^{208}Pb/^{204}Pb$ versus $^{206}Pb/^{204}Pb$. (c) $^{207}Pb/^{204}Pb$ versus $^{206}Pb/^{204}Pb$.

shield stage, then material that comprises slump blocks and debris should be primarily tholeiitic in composition. This is the case for samples collected from the Nu'uanu-Wailau landslide complex off Ko'olau and Moloka'i volcanoes [*Clague et al.*, 2002; *Shinozaki et al.*, 2002], the South Kona landslide off Mauna Loa [*Lipman et al.*, 2003], and Laupāhoehoe landslide off Kohala volcano (M. Coombs and J.-I. Kimura, unpublished data, 2002). Exceptions are the Hilina bench off the south flank of Kīlauea, which is composed of a mixture of alkalic debris from preshield Kīlauea with tholeiitic shoreline sands from Mauna Loa and Mauna Kea [*Lipman et al.*, 2002; *Sisson et al.*, 2002], and an elongate sliver of volcaniclastic debris at the base of Hualālai volcano, which contains a small amount of preshield alkalic material [*Hammer and Shamberger*, 2003]. Thus composition of landslide debris can provide information about the timing of slump and landslide emplacement relative to the growth stage of a given volcano.

[61] Pillow lavas and all but one hyaloclastite sample from the Wai'anae slump complex's outer bench (K205, S707) are compositionally similar tholeiites and suggest that Wai'anae Volcano is their source. The rocks are relatively unfractionated and low in incompatible elements and are thus similar to subaerially erupted lavas (Lualualei Member) from Wai'anae's early shield stage. In addition, isotope values for pillow lavas from S707 overlap with those reported for subaerial Wai'anae samples [*White and Hoffman*, 1982; *Stille et al.*, 1983]. Thus rocks that comprise the outermost portion of the Wai'anae slump complex erupted early in the volcano's shield stage.

[62] Glass sulfur contents can provide additional information about vent location. Tholeiite glasses from K205 all have low dissolved S, which is common for glasses within hyaloclastites from benches or landslide blocks, and indicates that these glasses erupted subaerially or very near sea level. Pillow rinds from S707 are also degassed, despite being sampled at >4000 m water depth. Degassed pillows have been found to water depths of 3100 m on the flank of Mauna Loa [*Davis et al.*, 2003], and up to 3300 m on Kīlauea's south flank [*Lipman et al.*, 2002]. In both cases, the pillows are interpreted as originating as subaerially erupted lavas that crossed the shoreline and traveled to their current water depth; in the case of Mauna Loa, edifice subsidence may have increased the water depth by up to 400 m [*Davis et al.*, 2003], but the degassed Kīlauea flow

is interpreted to be too young to have subsided significantly. The closest preserved ancient shoreline upslope from S707 is at 1800 mbsl, indicating that the S707 lavas traveled downslope >2 km from their source. On the basis of their location on a partially detached block, however, they may also have traveled some distance as a cohesive package, during postemplacement landsliding. Posteruptive flow, block slumping, and edifice subsidence all probably played a role in bringing the pillows to their current location near the base of the southeast bench. Directly upslope of site S707 is a break in slope and shelf at ~950 m water depth, between O‘ahu and Penguin Bank (Figure 1). Beneath this shelf may lie the submarine or partly subaerial extension of Wai‘anae’s south rift zone.

[63] Although tholeiite is the predominant composition sampled from the outer bench, a small amount of transitional material was recovered from K205. It is compositionally dissimilar to any lavas previously sampled on land at Wai‘anae, and its occurrence with relatively unfractionated tholeiites at the base of the slump suggests that it erupted early in the volcano’s history, not late. The S contents of the transitional glasses (200 to 550 ppm) bridge the value typically thought to delineate degassed, subaerially erupted lavas from submarine erupted ones [*Davis et al.*, 2003; *Dixon et al.*, 1991], suggesting that the transitional basalt grains may have erupted from a submarine vent. It is unlikely that the transitional grains are subaerial tephra, as they are nonvesicular. The occurrence of the grains in the same hyaloclastite clast in which completely degassed tholeiite grains are found suggests that the volcano may have erupted compositionally varied magmas at different vent locations within a short time span.

[64] T326 hyaloclastite glasses and breccia clasts from the upper northwestern block are also tholeiitic, but the compositions are more fractionated than those from deeper in the slump. They are similar to tholeiites exposed as dikes within Wai‘anae’s subaerial edifice, which are interpreted to have erupted late in Wai‘anae’s shield stage [*Zbinden and Sinton*, 1988] and overlap compositionally with late stage Kamaile‘unu Member lavas [*Guillou et al.*, 2000; J. Sinton, unpublished data]. Therefore, while material from early in the volcano’s shield stage is exposed at the toe of the slump, the upper portion is composed of younger material from Wai‘anae’s late shield stage. The S contents of glass grains from T326 are consistently lower than S contents of K205 tholeiite glasses. This may be due to longer travel distances from vent to shoreline for the lavas that fed the T326 hyaloclastites, allowing more complete degassing. This is consistent with T326 evolved tholeiites erupting late in Wai‘anae’s shield stage, when the subaerial edifice would have been larger and the vent further from shoreline. However, the abundant pillow lava clasts show that the block itself is predominantly composed of submarine-emplaced lava that was originally erupted subaerially. Thus the block must have originated from below the paleoshoreline, which upslope of the block is ~1400 mbsl.

[65] We found no materials within the slump that compositionally resemble postshield Palehue or Kolekole Member subaerial lavas. If slumping occurred between eruption of Palehue and Kolekole Member postshield lavas, as suggested by *Presley et al.* [1997], one might expect to find some Palehue material in the slump complex. Our sampling was by no means comprehensive, however, and postshield lavas were probably not as extensively emplaced as those erupted during the shield stage. Therefore we cannot conclude that slumping did or did not occur during this time interval. Further discussion of the timing of mass wasting events is discussed in a section 6.4.

6.2. Origins of Hyaloclastite and Core Glasses From North of Ka‘ena Ridge

[66] Glass grains dispersed within sediments collected during dives T327 and T328 on the north side of Ka‘ena Ridge are compositionally distinct from all other glasses collected for this study, and instead resemble lavas erupted from Ko‘olau volcano on the eastern half of O‘ahu. These glass grains are degassed and must have been derived from shoreline crossing lavas or explosive eruption from the younger volcano. A single grain from the sediment cores is alkalic and resembles glasses from T327 lithified hyaloclastites.

[67] Hyaloclastite clasts found within the mud during dive T327 contain glasses that are compositionally varied and more alkalic than others collected during the study. They may have derived from Wai‘anae’s late shield or postshield stage; they are similar to alkalic dike glasses sampled by *Zbinden and Sinton* [1988]. During dives T327 and T328, elevated heat flow was measured near large blocks, suggesting that these were outcrops, not talus or float [*Jordahl et al.*, 2001]. In this case, the

hyaloclastite samples from the dives are probably derived from in situ bedrock.

6.3. Wai‘anae’s Submarine Rift Zones

[68] The subaerial rift zones of Wai‘anae Volcano are defined by concentrations of subparallel dikes that trend to the northwest and to the south. Onshore, the two rift zones are ~18 and ~13 km long, respectively, but how far they extend beyond shoreline is not known. Ka‘ena Ridge has previously been mapped as the submarine extension of the northwest rift zone [*Holcomb and Robinson*, 2004]. The orientation of dikes that define the subaerial northwest rift zone [*Stearns*, 1939; *Zbinden and Sinton*, 1988] are oriented primarily parallel to Ka‘ena Ridge, consistent with this interpretation. Subaerial lavas exposed at Ka‘ena Point dip north, however, indicating that this topographic ridge is the remnant of the northern flank of the subaerial edifice, and not the rift zone axis (J. Sinton, written communication, 2004). Thus, if the submarine Ka‘ena Ridge is the extension of Wai‘anae’s northwest rift zone, the rift axis must lie to the south of Ka‘ena Point.

[69] The whole rock data for subaerial basalt clasts from dive T325 on the crest of Ka‘ena Ridge are too scattered to evaluate whether these lavas shared a common source with other Wai‘anae lavas. The upper northwestern block may have separated from the proximal Ka‘ena Ridge, and the similarity of T326 compositions to those of late-shield Wai‘anae lavas suggests that at least the proximal part of Ka‘ena Ridge formed as Wai‘anae’s rift zone. If the northwest rift zone does extend to the end of Ka‘ena Ridge, its total length would be ~80 km. This is comparable to Haleakalā’s east rift zone (140 km), Kīlauea’s east rift zone (120 km), and Mauna Loa’s southwest rift zone (100 km).

[70] Similarly, we cannot place precise constraints on the length of Wai‘anae’s south rift zone. It is likely, however, that the rift zone extends far enough to the south to provide the source for pillow lavas sampled during dive S707. On the basis of GLORIA imagery, *Holcomb and Robinson* [2004] have mapped the tip of a rift zone emerging from the southern end of the shelf. This may be a continuation of a rift zone beneath Penguin Bank from an obscured volcano. If instead it is the end of Wai‘anae’s south rift zone, the rift would be ~90 km long. Alternatively, a poorly defined positive Bouguer gravity anomaly extends to ~45 4kilometers SSE of Barbers Point [*Strange et al.*, 1965b] and may reveal the extent of the south rift zone. This would place the source of the S707 lavas near the 65 km-long rift zone’s tip.

6.4. Growth and Collapse of Wai‘anae Volcano

[71] Bathymetric data, dive observations, and compositions of samples collected during the dives suggest that Wai‘anae Volcano experienced multiple stages of deformation as it grew, including episodes of catastrophic slope failure, localized sector detachment, and probably a long-lived history of gravitational spreading. We recognize that the new data provide constraints on, but not a unique solution to, the volcano’s history. By coupling our data with models presented for better-studied Hawaiian volcanoes, we infer a series of events that plausibly marked the growth of Wai‘anae Volcano during its shield stage, with emphasis on events that modified its southwest flank.

[72] Wai‘anae’s peak shield building stage occurred at about 4–3 Ma, approximately a million years prior to that of its nearest neighbor, Ko‘olau volcano [*Clague and Dalrymple*, 1987; *Haskins and Garcia*, 2004]. Thus Wai‘anae Volcano probably underlies much of Ko‘olau’s edifice [*Fiske and Jackson*, 1972; *Moore and Clague*, 2002], and grew directly on the seafloor unimpeded by the presence of other volcanoes until late in its evolution. During its shield stage, the volcano developed two significant rift zones, one to the northwest and the other to the south.

[73] We suggest that by the end of the early shield stage, an extensive bench had formed on the volcano’s southwest flank (Figure 13a). Such benches exist on the flanks of many Hawaiian volcanoes, though they vary greatly in volume, extent, and morphology. It is generally agreed that gravitationally driven volcano spreading contributes to their formation, but their internal structure and thus the details of their formation are still debated. These benches may form as a result of landsliding of debris from the shallow submarine and subaerial flanks of the volcanic edifice, followed by modest compression and uplift during continued volcano spreading [*Lipman et al.*, 2002, 2003]. Alternatively, midslope benches may form as volcaniclastic debris, originally deposited as a more widespread apron on the seafloor, is offscraped and uplifted into stacked thrusts during volcano spreading [*Morgan et al.*, 2000; *Morgan and Clague*, 2003]. The subparallel ridges that comprise Wai‘anae’s outer bench may be more consistent with the latter model, if the ridges are

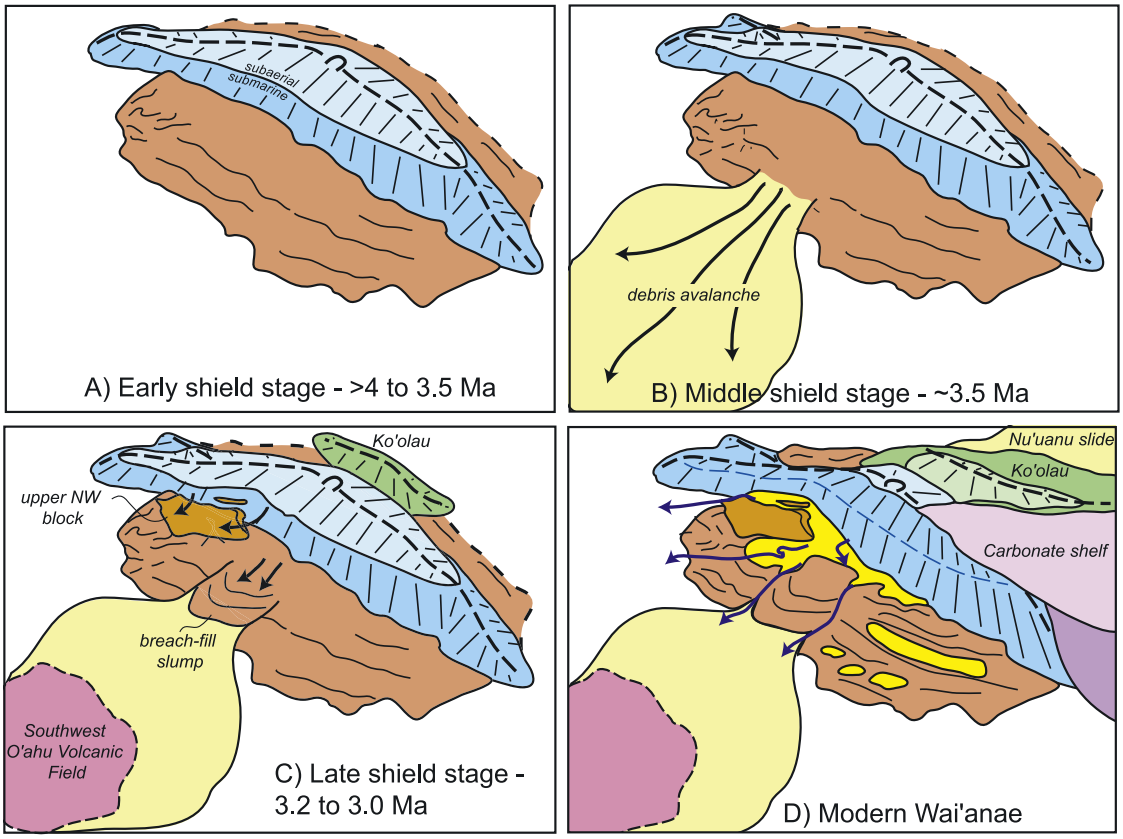

Figure 13. Schematic model of the evolution of Wai‘anae Volcano’s southwest flank. Dates are approximate and are taken from geochronology on subaerial shield stage lavas [*Guillou et al.*, 2000]. (a) During the early shield stage, high eruptive rates, extensive sedimentation of subaerially erupted material, volcano spreading, and gravitational slumping led to the formation of an extensive bench (shown in orange) on Wai‘anae’s southwest flank. The volcano had developed rift zones to the northwest and south, though their lengths are unknown. (b) After formation of the extensive slump bench, the middle shield stage was marked by a debris avalanche that breached the slump’s outer bench and deposited extensive debris on the sea floor southwest of the slump. (c) Late in the volcano’s shield stage, or after the end of shield building, an upper landslide block was emplaced above the northern slide, and the breach in the outer bench was filled by continued slumping in the central portion of the slump. Southwest O‘ahu Volcanic Field lavas were emplaced beginning at ~3 Ma [*Noguchi and Nakagawa*, 2003], and Ko‘olau started growing >2.9 Ma [*Haskins and Garcia*, 2004]. (d) Due to subsidence, much of the originally subaerial Wai‘anae edifice is below sea level (paleoshoreline shown by dashed blue line). Ko‘olau, which grew from >3 to ~2 Ma [*Haskins and Garcia*, 2004; *Clague and Dalrymple*, 1987], was built on Wai‘anae’s eastern shoulder. The areas south of O‘ahu have been filled in by carbonates, and the end of Wai‘anae’s south rift zone may have been covered by lavas erupted from Penguin Bank. Basins atop the Wai‘anae slump complex have filled in with sediment eroded from the volcano’s subaerial edifice (bright yellow), and channels (blue arrows) cut into sediment and form canyons that cut into the slump’s outer margin.

interpreted as thrust fronts. Critical observations that would differentiate between the two, such as seismic reflection data and extensive seafloor observations, are not currently available.

[74] After the formation of the bench, several gravitational slope failure events may have modified the volcano’s southwest flank. The hummocky region at the northern edge of the outer bench may be the site of one of these collapses (Figures 2a and 13b). The overall morphology of the area is similar to that of Pololū slump off the northeast flank of Kohala volcano, which has been interpreted to partially overlie the Laupahoehoe slump to the east in much the same fashion [*Smith et al.*, 2002]. Alternatively, this region may simply be a more chaotically emplaced section of the outer bench, or could be continuous with the upper northwestern block.

[75] The debris field on the seafloor southwest of the outer bench likely resulted from a debris

avalanche, based on its morphology and observations from dive S703 (Figures 2b and 13b). Debris slides such as this one are thought to form quickly and catastrophically [e.g., *Moore et al.*, 1989; *Lipman et al.*, 1988]. The timing and source region of the avalanche are not known. It could have occurred prior to formation of the main slump complex, as has been proposed for a debris field outboard of the midslope bench on Kīlauea's south flank [*Morgan et al.*, 2003]. Alternatively, the debris avalanche could have occurred after formation of the Wai‘anae's slump outer bench. The latter scenario seems most likely, as the portion of the debris field closest to the main slump is aligned with a distinct embayment in the outer bench. Also, the volume of the debris deposit is probably no more than 500 km^3, based on its area and an average thickness of <200 m. This volume would be roughly similar to the volume of material missing from the breach in the outer bench, prior to slumping that has partially refilled it. Thus the debris avalanche may have formed only from collapse of part of the outer bench, and was not headed in the shallow portion of the volcanic edifice. This is consistent with the compositions of hyaloclastite sampled during dive S703, which are relatively unfractionated tholeiites, similar to those found during dives on the outer bench.

[76] Several lines of evidence indicate that S703 lava as well as other Southwest O‘ahu Volcanic Field lavas postdate emplacement of the debris field on the seafloor, thus placing a further constraint on the timing of debris avalanche emplacement. 1) The lavas are clearly visible as bright, reflective regions in side scan sonar imagery [*Groome et al.*, 1997; *Holcomb and Robinson*, 2004]. 2) Sheet lava was observed overlying one of the S703 volcaniclastic mounds. 3) Lavas have thinner manganese oxide crusts ($\leq$3 mm) than volcaniclastic samples ($\leq$6 mm). Mn crusts on submarine Hawaiian rocks grow at a rate of approximately 2 mm $Ma^{-1}$and thus can be used as exposure geochronometers [*Moore and Clague*, 2004], suggesting ages of $\sim$3 Ma and 1.5 Ma for the S703 volcaniclastics and lavas, respectively. Alkalic lavas from another area of the Southwest O‘ahu Volcanic Field have been dated at $\sim$3 Ma [*Noguchi and Nakagawa*, 2003], suggesting that the volcanic field formed over a considerable time span, and that 3 Ma is a younger limit on the age of the debris field.

[77] After emplacement of the debris avalanche, the breach in the outer bench was apparently filled by continued slumping in the central portion of the slump. Increased deformation following release of buttressing material has been proposed along Kīlauea's south flank and the Kona region of Mauna Loa [*Morgan and Clague*, 2003; *Morgan et al.*, 2003], and a similar process may have occurred at Wai‘anae after collapse of a section of the outer bench. The timing of infilling of the breach is unknown, but would be expected to have occurred soon after unbuttressing.

[78] The upper northwestern landslide block was probably emplaced late in the volcano's shield stage, or later, atop the northern bench (Figures 2a and 13c). Two lines of evidence suggest that block movement either occurred late in the shield stage or after the end of shield building. First, as discussed above, the composition of volcaniclastics recovered from dive T326 on the upper block are similar to late-shield stage lavas of the Kamaile‘unu Member. Secondly, upslope of the upper block there is a marked break in slope that is much shallower than the slope break both along Ka‘ena Ridge to the west and beneath Wai‘anae's summit area to the southeast (Figure 1). The slope break upslope of the upper block is interpreted to be a headwall scarp for the displaced block rather than the transition from subaerial to submarine environments, as it is to either side. That this shallow scarp has been preserved suggests that it was above paleosealevel, and that subsequent eruptions did not fill in the scarp. Thus eruptive activity along that segment of the rift zone had largely ceased when collapse of the upper block occurred. No evidence is available to constrain the minimum emplacement age for the upper northwestern block.

[79] Active volcano growth ceased at $\sim$3 Ma, and it seems likely that most deformation of the volcano's flank had ceased by this time. Since then, subsidence has lowered much of the originally subaerial Wai‘anae edifice below sea level (Figure 13d). Ko‘olau, which grew from 3 to 2 Ma [*Clague and Dalrymple*, 1987], was built on Wai‘anae's eastern shoulder, adding to subsidence of the island. The area south of O‘ahu flanking Penguin Bank has been filled in by carbonate reefs, and the end of Wai‘anae's south rift zone may have been covered by lavas erupted from Penguin Bank. Structural basins atop Wai‘anae slump have been filled with sediment eroded from the volcano's subaerial edifice, and channels were cut by submarine density currents into sediment, forming canyons that also cut down

Table A1 (Representative Sample). Sample Descriptions (The full Table A1 is available in the HTML version of this article at http://www.g-cubed.org)

Sample	Rock Type, Collection Site	Composition/Texture	Depth, m	Latitude	Longitude	gl[a]	wr	is
K205-1a	lithified polymict breccia, float	olivine-rich glassy and crystalline basalt grains in palagonite matrix	4637	21.057	−158.633	x		
K205-1b	monomict hyaloclastite, float	olivine-rich glass grains in heavily palagonitized matrix	4637	21.057	−158.633	x		
K205-1c	lithified polymict breccia, float	olivine-rich glassy and crystalline basalt grains in palagonite/smectite matrix	4637	21.057	−158.633	x		
K205-2	lithified polymict breccia, from talus	crystalline grains in palagonite/zeolite matrix; glass grains replaced by palagonite	4612	21.057	−158.633	x		
K205-3a-1	monomict hyaloclastite, from talus	olivine-rich glass grains in heavily palagonitized matrix	4611	21.057	−158.633	x		
K205-3a-2	monomict hyaloclastite, from talus	olivine-rich glass grains in heavily palagonitized matrix	4611	21.057	−158.633	x		
K205-3a-3	polymict hyaloclastite, from talus	olivine-rich crystalline and glassy basalt grains in heavily palagonitized matrix; abundant zeolite-filled fractures	4611	21.057	−158.633	x		
K205-3b	lithified polymict breccia, from talus	olivine-rich crystalline and glassy basalt grains in heavily palagonitized matrix; abundant zeolite-filled fractures	4611	21.057	−158.633	x		
K205-3c-1	polymict hyaloclastite clast from unlithified polymict breccia, float	olivine-rich crystalline and glassy basalt grains in heavily palagonitized matrix; abundant zeolite-filled fractures	4611	21.057	−158.633	x		
K205-3c-2	lithified polymict breccia clast from unlithified polymict breccia, float	olivine-rich crystalline and glassy basalt grains in heavily palagonitized matrix; abundant zeolite-filled fractures	4611	21.057	−158.633	x		
K205-3c-3	lithified polymict breccia clast from unlithified polymict breccia, float	vesicular, crystalline olivine-rich basalt clast with adhering palagonitezed hyaloclastite matrix	4611	21.057	−158.633	x		
K205-3c-4	lithified polymict breccia clast from unlithified polymict breccia, float	olivine-rich crystalline and glassy basalt grains in heavily palagonitized matrix; abundant zeolite-filled fractures	4611	21.057	−158.633	x		
K205-3c-6	lithified polymict breccia clast from unlithified polymict breccia, float	olivine-rich crystalline basalt clasts in smectite/palagonite matrix	4611	21.057	−158.633			
K205-4	polymict hyaloclastite, from talus	glassy and crystalline grains in palagonite/zeolite matrix	4586	21.057	−158.632	x		
K205-5a	polymict hyaloclastite, from fractured outcrop	glassy and crystalline grains in palagonite/zeolite matrix	4560	21.058	−158.632	x		
K205-5b	polymict hyaloclastite, from fractured outcrop	glassy and crystalline grains in heavily palagonitized matrix	4557	21.058	−158.632	x		
K205-6	lithified polymict breccia, from fractured outcrop	glassy and crystalline grains in palagonite/zeolite matrix	4543	21.058	−158.631	x		
K205-7a	lithified polymict breccia, from talus at base of outcrop	olivine-rich glassy and crystalline basalt grains in palagonite/smectite matrix	4425	21.059	−158.631	x		
K205-7b	lithified polymict breccia, from talus at base of outcrop	olivine-rich crystalline and glassy basalt grains in heavily palagonitized matrix	4425	21.059	−158.631	x		
K205-7c	lithified polymict breccia, from talus at base of outcrop	olivine-rich crystalline and glassy basalt grains in heavily palagonitized matrix	4425	21.059	−158.631	x		

[a] The last three columns indicate analyses that have been performed for each sample: gl, EPMA of glass rinds or grains; wr, XRF and ICPMS of whole rock; is, isotopic analysis of whole rock.

the slump's outer margin before ending on the abyssal plain.

7. Concluding Remarks

[80] The data provided here on the submarine portion of Waiʻanae's edifice reveal much about the history of this Hawaiian volcano, though many questions still remain. On the basis of detailed bathymetry and correlation of sampled material to subaerial Waiʻanae lavas, Waiʻanae Volcano is larger than previously estimated, and including its rift zones extends out Kaʻena Ridge and to the south toward Penguin Bank, though how far is still unknown. Gravity and magnetic measurements could help constrain the full lengths of these rift zones. Unresolved questions also include the relation of the Waialu Ridge rift zone to Kaʻena Ridge and Waiʻanae Volcano. Further study of the slump, including dating of sampled materials, would provide more detailed constraints on the timing of collapse with respect to volcano growth.

[81] The Waiʻanae slump complex formed through a deformational history of relatively long-term mass movement punctuated by catastrophic collapse events, rather than as a single event. Most or all of the deformation of the flank probably occurred during or shortly after the volcano's tholeiitic shield stage, suggesting that high eruption and sedimentation rates played roles in driving deformation. The large majority of material recovered from the slump was erupted above sea level. These observations provide a framework for further work at this volcano, and indeed closer examination of the flanks of other Hawaiian volcanoes may reveal that their deformational histories hold much in common with that of Waiʻanae.

Appendix A

[82] Descriptions of samples collected during Waiʻanae area dives are provided in Table A1. For each sample, we indicate the rock type and site (talus, outcrop, etc.) and provide compositional and textural descriptions, sample locations, and analysis type (if applicable).

Acknowledgments

[83] We thank the crews of the JAMSTEC R/Vs *Kairei* and *Yokosuka* for their dedication during the 2001 and 2002 cruises, respectively. The skill of the operational teams of both *Kaiko* and *Shinkai* 6500 allowed diving operations to run smoothly. We thank the shipboard scientific parties for their contributions and discussions, especially S. Umino who acted as dive observer during Dive S703. We also thank Captain I. Young and the crew of the R/V *Western Flyer*, chief pilot D. Graves and the crew of the ROV *Tiburon*, and the science party on the *Western Flyer* during the final leg of MBARI's Hawaiʻi Expedition in 2001. R. Oscarson ably maintains the electron microprobe facility in Menlo Park. A. Davis performed some of the microprobe analyses, J. Paduan helped with sample preparation for whole rock analyses, and J. Robinson assisted with GIS data compilation. K. Jordahl allowed access to the cores collected for thermal conductivity measurements during dives T327 and T328. T. Kanamatsu helped us obtain bottom photographs for dive K205. J. Sinton generously provided unpublished data for subaerial shield stage Waiʻanae Volcano as well as useful comments on the manuscript. Reviews by B. Eakins, R. Fiske, and J. Moore are appreciated, and reviews by P. Lipman and J. Morgan were especially helpful. This work was supported by the USGS Volcano Hazards Program, Japan Marine Science and Technology Center, and the David and Lucile Packard Foundation.

References

Borgia, A., and B. Treves (1992), Volcanic plates overriding the ocean crust: Structure and dynamics of Hawaiian volcanoes, in *Ophiolites and Their Modern Oceanic Analogues*, edited by W. J. McGuire, A. P. Jones, and J. Nueberg, *Geol. Soc. Spec. Publ.*, *60*, 277–299.

Caress, D. W., and D. N. Chayes (1996), Improved processing of Hydrosweep DS multibeam data on the R/V *Maurice Ewing*, *Mar. Geophys. Res.*, *18*, 631–650.

Chadwick, W. W., Jr., J. R. Smith Jr., J. G. Moore, D. A. Clague, M. O. Garcia, and C. G. Fox (1993), Bathymetry of south flank of Kīlauea Volcano, Hawaiʻi, *U.S. Geol. Surv. Misc. Field Invest. Map*, *MF-2231*.

Clague, D. A., and G. B. Dalrymple (1987), The Hawaiian-Emperor volcanic chain; Part I, Geologic evolution, *U.S. Geol. Surv. Prof. Pap.*, *1350*, 5–73.

Clague, D. A., J. G. Moore, J. E. Dixon, and W. B. Friesen (1995), Petrology of submarine lavas from Kīlauea's Puna Ridge, Hawaiʻi, *J. Petrol.*, *36*, 299–349.

Clague, D., J. Moore, and A. Davis (2002), Volcanic breccia and hyaloclastite in blocks from the Nuʻuanu and Wailau landslides, Hawaiʻi, in *Hawaiian Volcanoes: Deep Underwater Perspectives*, *Geophys. Monogr. Ser.*, vol. 128, edited by E. Takahashi et al., pp. 279–296, AGU, Washington, D. C.

Clague, D. A., B. L. Cousens, J. E. Dixon, K. Hon, J. G. Moore, and J. R. Reynolds (2003), Submarine rejuvenated-stage lavas offshore Molokai, Oahu, Kauai, and Niihau, Hawaii, *Eos Trans. AGU*, *84*(46), Fall Meet. Suppl., Abstract V11B-01.

Cousens, B. L. (1996), Magmatic evolution of Quaternary mafic magmas at Long Valley Caldera and the Devils Postpile, California: Effects of crustal contamination on lithospheric mantle-derived magmas, *J. Geophys. Res.*, *101*, 27,673–27,689.

Davis, M. G., M. O. Garcia, and P. Wallace (2003), Volatiles in glasses from Mauna Loa Volcano, Hawaiʻi: Implications for magma degassing and contamination, and growth of Hawaiian volcanoes, *Contrib. Mineral. Petrol.*, *144*, 570–591.

Denlinger, R. P., and P. Okubo (1995), Structure of the mobile south flank of Kīlauea Volcano, Hawaii, *J. Geophys. Res.*, *100*, 24,499–24,507.

Dixon, J. E., D. A. Clague, and E. M. Stolper (1991), Degassing history of water, sulfur, and carbon in submarine lavas from Kīlauea Volcano, Hawai'i, *J. Geol.*, *99*, 371–394.

Eakins, B., and J. Robinson (2002), Multibeam bathymetry of Haleakala Volcano, Maui, *Eos Trans. AGU*, *83*(47), Fall Meet. Suppl., Abstract T62A-1294.

Fiske, R. S., and E. D. Jackson (1972), Orientation and growth of Hawaiian volcanic rifts: The effect of regional structure and gravitational stresses, *Proc. R. Soc. London*, *329*, 299–326.

Fornari, D., and J. F. Campbell (1987), Submarine topography around the Hawaiian Islands, *U.S. Geol. Surv. Prof. Pap.*, *1350*, 109–124.

Frey, F. A., M. Garcia, and M. F. Roden (1994), Geochemical characteristics of Ko'olau volcano: Implications of intershield geochemical differences among Hawaiian volcanoes, *Geochim. Cosmochim. Acta*, *58*, 1441–1462.

Frey, F. A., D. A. Clague, J. J. Mahoney, and J. Sinton (2000), Volcanism at the edge of the Hawaiian plume: Petrogenesis of submarine alkalic lavas from the North Arch Volcanic Field, *J. Petrol.*, *41*, 667–691.

Garcia, M., D. W. Muenow, K. E. Aggrey, and J. R. O'Neil (1989), Major element, volatile, and stable isotope geochemistry of Hawaiian submarine tholeiitic glasses, *J. Geophys. Res.*, *94*, 10,525–10,538.

Groome, M. G., C. E. Gutmacher, and A. J. Stevenson (1997), *Atlas of GLORIA Sidescan-Sonar Imagery of the Exclusive Economic Zone of the United States: EEZ-View* [CD-ROM], *U.S. Geol. Surv. Open File Rep.*, *97–540*.

Guillou, H., J. Sinton, C. Laj, C. Kissel, and N. Szeremeta (2000), New K-Ar ages of shield lavas from Wai'anae Volcano, O'ahu, Hawaiian Archipelago, *J. Volcanol. Geotherm. Res.*, *96*, 229–242.

Hammer, J. E., and P. J. Shamberger (2003), Dynamic submarine flanks of Hualalai Volcano, Hawaii, *Eos Trans. AGU*, *84*(46), Fall Meet. Suppl., Abstract V22C-0602.

Haskins, E. H., and M. O. Garcia (2004), Scientific drilling reveals geochemical heterogeneity within the Koolau shield, Hawaii, *Contrib. Mineral. Petrol.*, *147*, 162–188.

Holcomb, R. T., and J. E. Robinson (2004), Map of Hawaiian Island Exclusive Economic Zone interpreted from GLORIA sidescan-sonar imagery, *U.S. Geol. Surv. Sci. Invest. Map Ser.*, *2824*.

Hussong, D. M., J. F. Campbell, D. Hills, D. W. Peate, and J. Williams (1987), Detailed mapping of the submarine geology of O'ahu, Hawai'i, using the SeaMARC/S system, *Eos Trans. AGU*, *68*(44), Fall Meet. Suppl., 1336.

Jordahl, K., M. McNutt, and L. Christiansen (2001), Low heat flow values measured on the Hawaiian Ridge, *Eos Trans. AGU*, *82*(47), Abstract T12B-0914.

Langenheim, V. A. M., and D. A. Clague (1987), The Hawaiian-Emperor volcanic chain; Part II, Stratigraphic framework of volcanic rocks of the Hawaiian Islands, *U.S. Geol. Surv. Prof. Pap.*, *1350*, 55–84.

Lipman, P. W., W. R. Normark, J. G. Moore, J. B. Wilson, and C. E. Gutmacher (1988), The giant submarine Alika debris slide, Mauna Loa, Hawai'i, *J. Geophys. Res.*, *93*, 4279–4299.

Lipman, P. W., J. M. Rhodes, and G. B. Dalrymple (1990), The Ninole Basalt: Implications for the structural evolution of Mauna Loa Volcano, Hawai'i, *Bull. Volcanol.*, *53*, 1–19.

Lipman, P., T. Sisson, T. Ui, J. Naka, and J. Smith (2002), Ancestral submarine growth of Kīlauea volcano and instability of its south flank, in *Hawaiian Volcanoes: Deep Underwater Perspectives*, *Geophys. Monogr. Ser.*, vol. 128, edited by E. Takahashi et al., pp. 161–191, AGU, Washington, D. C.

Lipman, P., B. Eakins, and H. Yokose (2003), Ups and downs on spreading flanks of ocean-island volcanoes: Evidence from Mauna Loa and Kīlauea, *Geology*, *31*, 841–844.

Macdonald, G. A., and T. Katsura (1964), Chemical composition of Hawaiian lavas, *J. Petrol.*, *5*, 83–133.

Mark, R. K., and J. G. Moore (1987), Slopes of the Hawaiian Ridge: Volcanism in Hawai'i, *U.S. Geol. Surv. Prof. Pap.*, *1350*, 101–107.

McDonough, W. F., and S.-S. Sun (1995), The composition of the Earth, *Chem. Geol.*, *120*, 223–253.

McMurtry, G. M., P. Watts, G. J. Fryer, J. R. Smith, and F. Imamura (2004), Giant landslides, mega-tsunamis, and paleo-sea level in the Hawaiian Island, *Mar. Geol.*, *203*, 219–233.

Moore, J. G. (1987), Subsidence of the Hawaiian Ridge, *U.S. Geol. Surv. Prof. Pap.*, *1350*, 85–100.

Moore, J. G., and J. F. Campbell (1987), Age of tilted reefs, Hawai'i, *J. Geophys. Res.*, *92*, 2641–2646.

Moore, J. G., and D. A. Clague (2002), Mapping the Nu'uanu and Wailau landslides in Hawai'i, in *Hawaiian Volcanoes: Deep Underwater Perspectives*, *Geophys. Monogr. Ser.*, vol. 128, edited by E. Takahashi et al., pp. 223–244, AGU, Washington, D. C.

Moore, J. G., and D. A. Clague (2004), Hawaiian submarine Mn-Fe oxide crusts, a dating tool?, *Geol. Soc. Am. Bull.*, *116*, 337–347.

Moore, J. G., and D. L. Peck (1965), Bathymetric, topographic, and structural map of the south-central flank of Kīlauea Volcano, Hawai'i, *U.S. Geol. Surv. Misc. Geol. Invest., Map I-456*.

Moore, J. G., D. A. Clague, and W. R. Normark (1982), Diverse basalt types from Lō'ihi Seamount, Hawai'i, *Geology*, *10*, 88–92.

Moore, J. G., D. A. Clague, R. T. Holcomb, P. W. Lipman, W. R. Normark, and M. E. Torresan (1989), Prodigious submarine landslides on the Hawaiian ridge, *J. Geophys. Res.*, *94*, 17,465–17,484.

Morgan, J. K., and D. A. Clague (2003), Volcanic spreading on Mauna Loa volcano, Hawai'i: Evidence from accretion, alteration, and exhumation of volcaniclastic sediments, *Geology*, *31*, 411–414.

Morgan, J. K., G. F. Moore, D. J. Hills, and S. Leslie (2000), Overthrusting and sediment accretion along Kīlauea's mobile south flank, Hawai'i, from marine seismic reflection data, *Geology*, *28*, 667–670.

Morgan, J. K., G. F. Moore, and D. A. Clague (2003), Slope failure and volcanic spreading along the submarine south flank of Kīlauea volcano, Hawaii, *J. Geophys. Res.*, *108*(B9), 2415, doi:10.1029/2003JB002411.

Noguchi, N., and M. Nakagawa (2003), Geochemistry of submarine Southwest-O'ahu volcano, Hawai'i: New type of Hawaiian volcano?, paper presented at Goldschmidt Conference, Geochem. Soc. of Jpn., Kurashiki, Japan.

Presley, T. K., J. M. Sinton, and M. Pringle (1997), Postshield volcanism and catastrophic mass wasting of the Wai'anae volcano, O'ahu, Hawai'i, *Bull. Volcanol.*, *58*, 597–616.

Satake, K., J. R. Smith, and K. Shinozaki (2002), Three-dimensional reconstruction and tsunami model of the Nu'uanu and Wailau giant landslides, Hawai'i, in *Hawaiian Volcanoes: Deep Underwater Perspectives*, *Geophys. Monogr. Ser.*, vol. 128, edited by E. Takahashi et al., pp. 333–346, AGU, Washington, D. C.

Sherman, S. B., M. Garcia, and E. Takahashi (2002), Major element geochemistry of glasses in turbidites as source in-

dicators: Implications for the Nuʻuanu and Wailau giant submarine landslides, in *Hawaiian Volcanoes: Deep Underwater Perspectives*, *Geophys. Monogr. Ser.*, vol. 128, edited by E. Takahashi et al., pp. 263–278, AGU, Washington, D. C.

Shinozaki, K., Z.-Y. Ren, and E. Takahashi (2002), Geochemical and petrological characteristics of Nuʻuanu and Wailau landslide blocks, in *Hawaiian Volcanoes: Deep Underwater Perspectives*, *Geophys. Monogr. Ser.*, vol. 128, edited by E. Takahashi et al., pp. 297–310, AGU.

Sinton, J. (1986), Revision of stratigraphic nomenclature of Waiʻanae volcano, Oʻahu, Hawaiʻi, *U.S. Geol. Surv. Bull.*, *1775-A*, A9–A15.

Sisson, T., P. Lipman, and J. Naka (2002), Submarine alkalic through tholeiitic shield-stage development of Kīlauea volcano, Hawaiʻi, in *Hawaiian Volcanoes: Deep Underwater Perspectives*, *Geophys. Monogr. Ser.*, vol. 128, edited by E. Takahashi et al., pp. 193–219, AGU, Washington, D. C.

Smith, J., K. Satake, J. Morgan, and P. Lipman (2002), Submarine landslides and volcanic features on Kohala and Mauna Kea volcanoes and the Hana Ridge, Hawaiʻi, in *Hawaiian Volcanoes: Deep Underwater Perspectives*, *Geophys. Monogr. Ser.*, vol. 128, edited by E. Takahashi et al., pp. 11–28, AGU, Washington, D. C.

Smith, J. R. (2002), The Keana Ridge submarine rift zone off Oahu, Hawaii, *Eos Trans. AGU*, *83*(47), Fall Meet. Supp., Abstract T62A-1300.

Smith, J. R., A. Malahoff, and A. N. Shor (1999), Submarine geology of the Hilina slump and morpho-structural evolution of Kīlauea volcano, Hawaiʻi, *J. Volcanol. Geotherm. Res.*, *94*, 59–88.

Stearns, H. T. (1939), Geologic map and guide of Oʻahu, Hawaiʻi, *Haw. Div. Hydrogr. Bull.*, *2*, 1–75.

Stearns, H. T. (1946), *Geology of the Hawaiian Islands*, *Haw. Div. Hydrogr. Bull.*, *8*, 106 pp.

Stille, P., D. M. Unruh, and M. Tatsumoto (1983), Pb, Sr, Nd, and Hf isotopic evidence of multiple sources for Oʻahu, Hawaiʻi basalts, *Nature*, *304*, 25–29.

Strange, W. E., L. F. Machesky, and G. P. Woollard (1965a), A gravity survey of the island of Oʻahu, Hawaiʻi, *Pac. Sci.*, *19*, 350–353.

Strange, W. E., G. P. Woollard, and J. C. Rose (1965b), An analysis of the gravity field over the Hawaiian Islands in terms of crustal structure, *Pac. Sci.*, *19*, 381–389.

Sun, S.-S., and W. F. McDonough (1989), Chemical and isotopic systematics of oceanic basalts: Implications for mantle composition and processes, in *Magmatism in Ocean Basins*, edited by A. D. Saunders and M. J. Norry, *Geol. Soc. Spec. Publ.*, *42*, 313–345.

Takahashi, E., et al. (2001), A newly recognized shield volcano southwest of Oahu Island, Hawaii, *Eos Trans. AGU*, *82*(47), Fall Meet. Suppl., Abstract V12B-0981.

Takahashi, E., et al. (2002), JAMSTEC Hawaii Cruise Report [CD-ROM], Jpn. Mar. Sci. and Technol. Cent., Yokosuka.

Tanaka, R., E. Nakamura, and E. Takahashi (2002), Geochemical evolution of Koʻolau volcano, Hawaiʻi, in *Hawaiian Volcanoes: Deep Underwater Perspectives*, *Geophys. Monogr. Ser.*, vol. 128, pp. 311–332, edited by E. Takahashi et al., AGU, Washington, D. C.

Todt, W., R. A. Cliff, A. Hanser, and A. W. Hofmann (1984), ^{202}Pb-^{205}Pb spike for Pb isotopic analysis, *Terra Cognita*, *4*, 209.

Walton, A. W., and P. Schiffman (2003), Alteration of hyaloclastites in the HSDP 2 Phase 1 Drill Core: 1. Description and paragenesis, *Geochem. Geophys. Geosyst.*, *4*(5), 8709, doi:10.1029/2002GC000368.

Ward, S. N. (2001), Landslide tsunami, *J. Geophys. Res.*, *106*, 1201–1215.

White, W. M., and A. W. Hoffman (1982), Sr and Nd isotope geochemistry of oceanic basalts and mantle evolution, *Nature*, *296*, 821–825.

Wolfe, E. W., W. S. Wise, and G. B. Dalrymple (1997), The geology and petrology of Mauna Kea Volcano, Hawaiʻi—A study of postshield volcanism, *U.S. Geol. Surv. Prof. Pap.*, *1557*, 129 pp.

Wright, T. L. (1971), Chemistry of Kīlauea and Mauna Loa lavas in space and time, *U.S. Geol. Surv. Prof. Pap.*, *735*, 40 pp.

Yokose, H., and P. Lipman (2004), Emplacement mechanisms of the South Kona submarine slide complex, Hawaiʻi Island: Observations by ROV Kaiko, *Bull. Volcanol.*, in press.

Zbinden, E. A., and J. M. Sinton (1988), Dikes and the petrology of Waiʻanae volcano, Oʻahu, *J. Geophys. Res.*, *93*, 14,856–14,866.